# Myosin Light Chain-2 Mutation Affects Flight, Wing Beat Frequency, and Indirect Flight Muscle Contraction Kinetics in *Drosophila*

**Jeffrey Warmke,* Mineo Yamakawa,‡ Justin Molloy,‡ Scott Falkenthal,* and David Maughan‡**

*Department of Molecular Genetics, The Ohio State University, Columbus, Ohio 43210; and ‡Department of Physiology and Biophysics, University of Vermont, Burlington, Vermont 05405

***Abstract.*** We have used a combination of classical genetic, molecular genetic, histological, biochemical, and biophysical techniques to identify and characterize a null mutation of the myosin light chain-2 (MLC-2) locus of *Drosophila melanogaster*. *Mlc2*$^{E38}$ is a null mutation of the MLC-2 gene resulting from a nonsense mutation at the tenth codon position. *Mlc2*$^{E38}$ confers dominant flightless behavior that is associated with reduced wing beat frequency. *Mlc2*$^{E38}$ heterozygotes exhibit a 50% reduction of MLC-2 mRNA concentration in adult thoracic musculature, which results in a commensurate reduction of MLC-2 protein in the indirect flight muscles. Indirect flight muscle myofibrils from *Mlc2*$^{E38}$ heterozygotes are aberrant, exhibiting myofilaments in disarray at the periphery. Calcium-activated Triton X-100–treated single fiber segments exhibit slower contraction kinetics than wild type. Introduction of a transformed copy of the wild type MLC-2 gene rescues the dominant flightless behavior of *Mlc2*$^{E38}$ heterozygotes. Wing beat frequency and single fiber contraction kinetics of a representative rescued line are not significantly different from those of wild type. Together, these results indicate that wild type MLC-2 stoichiometry is required for normal indirect flight muscle assembly and function. Furthermore, these results suggest that the reduced wing beat frequency and possibly the flightless behavior conferred by *Mlc2*$^{E38}$ is due in part to slower contraction kinetics of sarcomeric regions devoid or partly deficient in MLC-2.

FORCE production in virtually all types of muscle requires the formation of mechanically strained, elastic cross-bridges between myosin- and actin-containing filaments. These cross-bridges are composed of the globular heads of the myosin heavy chain subunits and their associated light chains (the myosin alkali light chain and the myosin light chain-2 (MLC-2)[1], the regulatory light chain). The myosin cross-bridge projects out from the thick (myosin) filament and attaches to an adjacent thin (actin) filament, activating an actomyosin $Mg^{2+}$-ATPase, which provides the chemical energy required for muscle contraction (Adelstein and Eisenberg, 1980). The cyclic making and breaking of these cross-bridges, together with a conformational change within the myosin molecule, causes the actin and myosin filaments to slide past each other enabling the muscle to shorten against an external load (Huxley, 1969).

Dr. Warmke's current address is Laboratory of Genetics, University of Wisconsin-Madison, Madison, WI 53706.

Dr. Yamakawa's current address is Bockus Research Institute, The Graduate Hospital, One Graduate Plaza, Philadelphia, PA 19146.

Dr. Molloy's current address is Department of Biology, University of York, Heslington, York Y01 5DD UK.

Address correspondence to Jeffrey Warmke at Laboratory of Genetics, 445 Henry Mall, University of Wisconsin-Madison, Madison, WI 53706.

1. *Abbreviations used in this paper*: IFM, indirect flight muscle; MLC-2, myosin light chain-2.

Two independent systems regulate the actomyosin ATPase cycle and contraction: a thin filament control system regulated by the troponin-tropomyosin complex, and a thick filament control system modulated by MLC-2 (Lehman and Szent-Gyorgyi, 1975; Sweeney and Stull, 1990, and references therein). The sophisticated molecular and genetic manipulations possible in *Drosophila* provides a powerful approach with which to investigate the structure-function relationships of these regulatory proteins (Peckham et al., 1990; Fyrberg and Beall, 1990). Our efforts have been directed toward defining the role of the MLC-2 protein. Here, we report the effects that altered MLC-2 stoichiometry have on myofibrillar structure, assembly and contraction.

In *Drosophila*, sarcomeric MLC-2 is encoded by a single gene (*Mlc2*) which maps to polytene chromosome bands 99E1-3 (Parker et al., 1985; Toffenetti, et al., 1987). *Mlc2* encodes a single protein isoform which is expressed in all muscle types throughout development. An initial step has been to identify a MLC-2 null mutation which can be used to analyze the effects of altered MLC-2 stoichiometry and to serve as a host strain for future analyses of in vitro mutagenized genes. To this end, we previously reported the molecular and genetic analysis of the 99D3 to 99E2-3 interval of the third chromosome and the identification of a putative MLC-2 mutation, *Ifm(3)99Eb*$^{E38}$ (Warmke et al., 1989).

*Ifm(3)99Eb*$^{E38}$, a recessive lethal mutation, was provi-

sionally deemed a hypomorphic allele of the MLC-2 gene for the following reasons: (*1*) *Ifm(3)99Eb*$^{E38}$ maps cytologically to the same region as the MLC-2 gene; (*2*) *Ifm(3)99Eb*$^{E38}$ defines the only dominant flightless complementation group (*Ifm(3)99Eb*) uncovered by a deficiency lacking the MLC-2 gene; (*3*) the flightless behavior of *Ifm(3)99Eb*$^{E38}$ is rescued by a duplication carrying a wild-type copy of *Ifm(3)99Eb*; (*4*) of 26 loci that are expressed at high concentration during myogenesis, only the MLC-2 gene is located in the 99D3 to 99E2-3 region (Falkenthal et al., 1984); and (*5*) MLC-2 gene expression is decreased in the thoracic musculature of adult *Ifm(3)99Eb*$^{E38}$ heterozygotes (Warmke et al., 1989).

Here we show the following: (*1*) *Ifm(3)99Eb*$^{E38}$ (denoted *Mlc2*$^{E38}$) corresponds to the MLC-2 gene by rescuing the *Mlc2*$^{E38}$ mutant phenotypes and mapping the *Mlc2*$^{E38}$ lesion within the MLC-2 locus. (*2*) *Mlc2*$^{E38}$ heterozygotes exhibit a reduced concentration of MLC-2 protein in the indirect flight muscles (IFMs). (*3*) Myofibrils from *Mlc2*$^{E38}$ heterozygotes are composed of approximately the same number of filaments as wild type; however, all IFM myofibrils of *Mlc2*$^{E38}$ heterozygotes show peripheral disruption. (*4*) *Mlc2*$^{E38}$ heterozygotes are severely flight impaired, yet have the ability to beat their wings but at a frequency that is ~30% less than that of wild-type flies. (*5*) Single IFM fibers, skinned with detergent and activated with $Ca^{2+}$, have maximum work outputs that occur at a lower oscillation frequency in *Mlc2*$^{E38}$ heterozygotes than in wild type flies. Together, these results suggest that the reduced wing beat frequency (and the corresponding flightless behavior) exhibited by *Mlc2*$^{E38}$ heterozygotes may be due at least in part to the slower contraction kinetics exhibited by their IFMs. We conclude that wild-type MLC-2 stoichiometry is required for normal indirect flight muscle assembly and function.

## Materials and Methods

### Fly Stocks and Culture Conditions

The *Ifm(3)99Eb*$^{E38}$ mutation was obtained in the laboratory of Dr. John Merriam (University of California at Los Angeles, Los Angeles, CA) from a screen for EMS-induced recessive lethal mutations as previously described (Warmke et al., 1989). Third chromosome balancers used are *In(3LR)TM3, ri p*$^{p}$ *sep su(Hw)*$^{2}$ *Sb bx*$^{34e}$ *e* and *In(3LR)TM6B, Hu e Tb ca* (Craymer, 1984), and will be referred to as *TM3,Sb* and *TM6B,Tb*, respectively. Other mutations and balancers used are described in Lindsley and Grell (1968) and Lindsley and Zimm (1985, 1987). Unless otherwise indicated, all fly stocks and crosses were maintained at room temperature (22°C) on agar-cornmeal based medium (Lewis, 1960).

### Flight and Wing Beat Testing

To determine flight indices, adult flies were collected within 24 h of eclosion, were aged for 2–4 d, and were tested individually using a graduated Benzer cylinder (Benzer, 1973). For the Benzer test, adult flies were dropped into a glass graduated cylinder coated with mineral oil. Gradations on the tube ranged from 8 at the top of the cylinder to 1 at the bottom. Flies that dropped straight through the cylinder were scored as 0. ~25–50 flies of a particular genotype were scored, and a flight index was determined by totaling the scores of each fly tested and dividing by the total number of flies tested.

For wing beat analysis, individual flies were flight tested then tethered and wing movement recorded by an optical device (modified from Unwin and Ellington, 1979). Frequency components were extracted using a spectrum analysis routine. For this analysis, the flight test consisted of simply determining whether the fly was capable of gaining elevation at least once in ten trials. Each fly was tapped out of a glass containment cylinder into the center of a lucite box. Flies that flew above the horizontal plane from which they were launched were scored U and were considered wild-type fliers. Nonfliers and weak fliers cannot gain elevation and were scored D. Flies tested using this method could be recovered and tested for wing beat frequency and dissected for single muscle fiber experiments.

### Construction of P Element Transformation Vectors, P Element Transformation, and Analysis of Transformed Lines

The P element transformation vector CaSpeR was provided by Dr. Vincenzo Pirrotta (Baylor College of Medicine, Houston, TX) and was constructed by inserting the 4.1-kb white minigene from BmD-w (Pirrotta et al., 1985) into the polylinker of Carnegie 4 (Rubin and Spradling, 1983). The MLC-2 transformation vector pCasJW1 was constructed by inserting a 3.4-kb EcoRI/HindIII fragment containing the entire MLC-2 transcription unit plus 700 bp of 5′ flanking sequences and ~650 bp of 3′ flanking sequences into CaSpeR. Likewise, pCasJW3 was constructed by inserting a 5.9-kb BclI/HindIII fragment containing the entire MLC-2 transcription unit plus 3.2 kb of 5′ flanking sequences and ~650 bp of 3′ flanking sequences into CaSpeR. The MLC-2 gene is the only transcription unit present in the sequences used to construct these transformation vectors (Parker et al., 1985; Toffenetti et al., 1987).

Microinjection and P element–mediated germline transformation were performed using a stable genomic source of P element transposase, *P[ry*$^{+}$ *Δ2-3] (99B)*, as described previously (Robertson et al., 1988). Chromosome linkage was determined for a number of independent transformants, and either a balanced lethal or a homozygous stock for each transformed line was established using standard genetic techniques.

### Cloning the Mlc2$^{E38}$ Allele

Because *Mlc2*$^{E38}$ is recessive lethal, it was necessary to clone the *Mlc2*$^{E38}$ allele from a library constructed from *Mlc2*$^{E38}$ heterozygotes. To facilitate identification of the *Mlc2*$^{E38}$ allele, it was necessary to identify a restriction site polymorphism between the *Mlc2*$^{E38}$ allele and a wild-type allele. Whole genomic Southern blot analysis of various wild-type and mutant stocks revealed that a PstI restriction site located approximately 950 bp 5′ of the transcription start site of the wild-type MLC-2 allele (*Mlc2*$^{+}$) of Canton-S is absent in the *Mlc2*$^{E38}$ allele (data not shown; Warmke, 1990). Therefore, the absence of this site could be used to identify *Mlc2*$^{E38}$ clones from a genomic library constructed with DNA isolated from *Mlc2*$^{E38}$/*Mlc2*$^{+}$ heterozygotes. Such a library ($6.4 \times 10^4$ recombinants) was screened by plaque hybridization (Benton and Davis, 1978) using a 5.9-kb BclI/HindIII restriction fragment that contains the entire MLC-2 transcription unit (Warmke, 1990) to isolate clones carrying MLC-2 sequences. Those carrying the *Mlc2*$^{E38}$ allele were identified by the PstI restriction site polymorphism. A 6.3-kb SalI/HindIII fragment of one clone (which contains the *Mlc2*$^{E38}$ allele) was subcloned into the Bluescript M13+ vector (Stratagene Corp., La Jolla, CA) and denoted pBSTE1. The Sequenase Version 2.0 DNA sequencing kit (United States Biochemical, Cleveland, OH) was used for all DNA sequencing reactions. Double stranded sequencing reactions were run essentially as described in the kit except that all termination reactions were done at 45°C. The products of all DNA sequencing reactions were displayed on 80 cm, 8 M urea–8% polyacrylamide gels. pBSTE1 (*Mlc2*$^{E38}$) and pLP5734 (wild-type MLC-2 allele from Canton-S; Parker et al., 1985) were used as templates. The noncoding strand of each plasmid DNA template was sequenced using synthetic oligonucleotide primers derived from the wild-type Canton-S sequence (Parker et al., 1985). To sequence the coding strand, the 2.2-kb PstI/HindIII fragments from pBSTE1 and pLP5734 were subcloned into Bluescript M13(+) and were denoted pBSTE-P/H2.2 and pBSTC-P/H2.2, respectively. The M13 universal primer was used to sequence pBSTE-P/H2.2 and pBSTC-P/H2.2.

### Electron Microscopy

Thoraces from 2-day-old adult flies and stage P14 pupae (according to Bainbridge and Bownes, 1981) were isolated by dissection in fixation buffer (3% paraformaldehyde, 3% glutaraldehyde, 0.1 M sucrose, 0.1 M sodium phosphate, pH 7.2, 0.002 M EGTA). Pupae were removed from the pupal case by first teasing away the anterior end of the pupal case. Then each pupa was pulled out of the pupal case with forceps by grasping onto the head of the animal. Thoraces were dissected by carefully removing the head, abdomen, and legs with forceps; special care was taken to avoid disrupting thoracic musculature when these tissues were removed. Following dissection, the

thoraces were incubated in fixation buffer for 3 h at room temperature. Then the samples were washed three times for 10 min each with wash buffer (0.1 M sucrose, 0.1 M sodium phosphate, pH 7.2) and postfixed in 1% osmium tetroxide, 0.1 M sodium phosphate, pH 7.2 for 1 1/2 h at room temperature. The samples were washed three times for 10 min each with wash buffer then dehydrated in a graded acetone series (10 min each in 30, 50, 70, 80, and 85%; two changes of 10 min each in 95%; two changes of 10 min each in 100%). The samples were embedded in Spurr low viscosity embedding medium (no. 21230; Polysciences, Inc., Warrington, PA) by incubating in 50% Spurr, 50% acetone overnight at room temperature; in 100% Spurr, two changes of 2 h each at room temperature; then transferred to gelatin capsules and polymerized at 60°C overnight. The blocks were trimmed and sectioned using a MT-2 Sorvall ultramicrotome (Sorvall Instruments, Newton, CT). Thick sections (~1 μm) were cut and stained with 1% Toludine blue and observed by light microscopy to confirm the orientation of the sample within the block and determine the location of the section of dorsal longitudinal muscle fibers within the thorax. The appropriate gold sections (~100 Å) were collected and stained with 2% uranyl acetate for 15 min then lead citrate for 3 min. Sections were viewed and photographed using a Phillips 300 electron microscope.

Single skinned fibers were fixed at room temperature in 2.5% glutaraldehyde, 10 mM $MgCl_2$, 20 mM MOPS buffer (pH 6.8) for 15 min, then transferred to the same solution with 0.2% tannic acid for 30 min. The preparation was rinsed with 20 mM MOPS (pH 6.8) for 15 min and 0.1 M phosphate buffer (pH 6.8) for 15 min. Fibers were postfixed, dehydrated, embedded, sectioned, and photographed according to protocols similar to those above. The average number of thick filaments per myofibril was determined by counting the number of thick filaments per myofibril in at least three myofibrils from at least three different adults for each stock.

## Separation of Protein Fractions and Gel Electrophoresis

Single fibers of the dorsal longitudinal indirect flight muscle, representative of those used in the functional assays, were isolated from the thorax under water-saturated mineral oil in a glass-bottom dish. Oil temperature was maintained at 7 ± 1°C by a Peltier device (Cambion; Cambridge Thermionic Corp., Cambridge, MA). Widths and lengths of segments were measured under the oil using a filar micrometer (LaSico, Los Angeles, CA) and binocular dissecting microscope (M5, Wild Heerbrugg, Rockleigh, NJ).

The relationship between MLC-2 gene dosage and expression in the IFM was examined by quantitative polyacrylamide gel electrophoresis. IFM proteins were separated into distinct cytosolic, organelle (mitochondria and sarcoplasmic reticulum) and cytomatrix fractions by procedures described below. The cytoplasmic fractionation procedure allowed the recovery of diffusible proteins that would otherwise be lost during the dissection or detergent treatment of the single fibers. Clearing the cytosolic and mitochondrial proteins from the individual IFM fibers also reduced the possibility that other proteins of similar mobility contributed to the stain densities attributed to MLC-2. A fiber was split, then transferred sequentially under oil through two 10-μl drops of relaxing solution [pCa 8($[Ca^{2+}] = 10)^{-8}$ M), 18 mM MgATP, 1 mM free $Mg^{2+}$, 5 mM EGTA, 20 mM BES buffer (pH 7.0), 150 mM ionic strength (adjusted with K methane sulfonate)], the second drop also contained 0.5% w/v Triton X-100. In some cases, fibers were transferred through drops of rigor solution instead of relaxing solution (rigor solution was similar in composition to relaxing solution, except ATP was omitted). Fibers remained in the first drop for 20 min, to allow all readily diffusible proteins (mostly arginine kinase and glycolytic enzymes) to diffuse out of the fiber. During the 30-min detergent treatment in the second drop, mitochondria and sarcoplasmic reticulum were solubilized and their protein constituents were allowed to diffuse out of the fiber. In some experiments, the fibers were rinsed for 2 min in 10 μl of relaxing or rigor solution after each extraction treatment.

For one-dimensional SDS-PAGE, each fiber was removed and sonicated in the appropriate buffer. A third of each drop into which proteins diffused was combined with SDS-sample buffer, and each fraction was then loaded into wells of a polyacrylamide slab gel (3.5% stacking, 15% running) for electrophoresis. Electrophoresis was carried out using a discontinuous buffer system (Giulian et al., 1983). Protein bands were silver stained (as in Giulian et al., 1983) and densities measured using a Shimadzu densitometer (model CS-930; Shimadzu Scientific Instruments, Columbia, MD).

For two-dimensional gel electrophoresis, samples were loaded onto a modified vertical focusing gel containing mixed ampholytes of pH range 4–7 (Giulian et al., 1984, their Table 1, native conditions). Two lanes from the focusing gels were cut out and applied end-to-end on the top of a SDS slab gel, and run as above. Protein standards were also run in a separate lane at the side. The two-dimensional gels were stained with silver as above and densities measured using the Shimadzu densitometer.

A number of proteins were identified tentatively by comparing the electrophoretic mobility of each band with those of purified protein standards from rabbit muscle (Sigma Chemical Co., St. Louis, MO). MLC-2 was identified by western blot analysis using purified rabbit anti-*Drosophila* MLC-2 sera (M. Graham, R. Tohtong, M. Chun, and S. Falkenthal, manuscript in preparation). For immunoblot analysis, proteins from SDS polyacrylamide (15%) gels were transferred to a nitrocellulose membrane and electroblotted using a Hoefer TE SemiPhor Transfer Unit. The membranes were blocked with standard Tris-buffer (pH 8.3) containing 3% w/v gelatin, rinsed in Tris-buffer (pH 8.3) containing 0.05% Tween-20 and incubated with buffer solution containing MLC-2-specific rabbit IgG (1:1,000) and actin-specific rat IgG (1:100). After washing in the Tween-20 containing buffer, the membranes were incubated with goat anti-rabbit IgG conjugated to avidin-horseradish peroxidase (1:3,000) and goat anti-rat IgG peroxidase conjugate (1:2,200). The peroxidase was then developed with Bio-Rad HRP color development reagent according to the manufacturer's instructions.

## IFM Mechanics and ATPase Measurements

Single fibers of dorsal longitudinal indirect flight muscle were isolated from the thorax. Immediately after the isolation, fibers were incubated for 3 h (8°C) in an extraction solution which solubilized surface membranes and organelles (50% glycerol v/v, 20 mM phosphate buffer, 1 mM sodium azide, 1 mM DTT, 2 mM $MgCl_2$, 0.5% w/v Triton X-100, pH 7.0). The skinned fibers were transferred to a temperature controlled trough containing relaxing solution (see above), and then attached to a force transducer (sensitivity, 0.6 μN/mV; natural frequency, 4 kHz) and a length controller (model 6000; Cambridge Tech., Watertown, MA) via aluminum T-clips (Goldman and Simmons, 1984). Sinusoidal length perturbations of 0.25% fiber length (peak-to-peak) and 1–500 Hz were applied. Both length and force transients were monitored with an oscilloscope and digitized by an A/D system (model DT-2828; Data Translations, Marlboro, MA). Fiber dimensions were measured using an inverted compound microscope. To measure steady active tension levels and complex stiffness, resting strain was set to near zero (White et al., 1988). For the ATPase measurement, strain in the active fiber was adjusted to yield maximum work output based on complex stiffness measurements. To activate the skinned fibers, relaxing solution (pCa 8, $[Ca^{2+}] = 10^{-8}$ M) was replaced with activating solution (pCa 4, $[Ca^{2+}] = 10^{-4}$ M). Later, rigor was induced by replacing the activating solution with an ATP-free solution (similar to relaxing solution, except MgATP was omitted).

Diffusion limitation of substrate availability was tested under conditions in which the bathing solution was not stirred (10 μl fiber solution under oil). At 12°C, muscle stiffness, stretch activation kinetics, and isometric ATPase were independent of phosphogen (MgATP) concentration above 15 mM (data not shown). Therefore, experiments were conducted at 12°C and 18 mM ATP to avoid or reduce the possibility of diffusion limitation of substrate. ATP hydrolysis was estimated from the resultant buildup of ADP in 10-μl drops of relaxing or activating solutions. To ensure that ADP production from each fiber was tightly linked with myosin ATP hydrolysis, a cocktail of inhibitors was added to the incubation solution: 10 μM diadenosine pentaphosphate to inhibit adenylate kinase (Leinhard and Secemski, 1973), quercitin to inhibit sarcoplasmic reticular ATPase, azide and oligomycein to inhibit mitochondrial ATPase (Cross and Boyer, 1975). Fibers were incubated in the test drops for 10–20 min, after which the ADP concentration in each drop was measured using high performance liquid chromatography (model 6000A solvent delivery system and model 440 absorbance detector; Waters, Milford, MA).

AMP, ADP, and ATP were separated on a reverse phase column (Biophase ODS, 5 μm; Bioanalytical Systems, West Lafayette, IN) as described by Victor et al. (1987). Two μl of experimental solution were mixed with 13 μl of running buffer and injected into a 20-μl sample loop (7125 sample injector, Rheodyne, Cotati, CA). Optical absorbance was measured at 254 nm, and all peaks were detected within 10 minutes of sample injection (pump speed, 3 ml/min, running buffer, pH 4.0). ATP/ADP concentration ratios were determined from the peak heights (after making a peak height adjustment for retention times).

"No-fiber" control drops were also analyzed and any background hydrolysis subtracted. Fiber myosin subfragment 1 (S1) content was determined

by calibrated densitometry of SDS-PAGE one-dimensional gels run on the single fiber preparations.

## Results

### *Identification of a Myosin Light Chain-2 Null Mutation*

*Ifm(3)99Eb*$^{E38}$ confers a significant decrease in flight ability (Table I); in fact, *Ifm(3)99Eb*$^{E38}$ heterozygotes do not fly but can produce wing movements to break their fall. To test whether the flightless behavior of *Ifm(3)99Eb*$^{E38}$ heterozygotes is due to a mutation in the MLC-2 locus (Warmke et al., 1989), we introduced a transformed copy of the wild-type MLC-2 gene to see if the dominant flightless behavior and recessive lethality conferred by *Ifm(3)99Eb*$^{E38}$ could be rescued.

P element-mediated germline transformation was used to generate a series of independent lines carrying an additional copy of the wild-type MLC-2 gene (see Materials and Methods). 15 independent lines carrying a transformed copy of the wild-type MLC-2 gene (*P[w*$^+$ *MLC-2*$^+$*]*) were recovered and characterized (Table I). Each transformed line was crossed to *Ifm(3)99Eb*$^{E38}$ heterozygotes, as outlined in Fig. 1. The resulting *Ifm(3)99Eb*$^{E38}$ heterozygotes that carry a transformed copy of the wild type MLC-2 gene were collected, and their flight behavior was determined. Three of the four inserts generated from the transformation vector pCasJW3 and ten of the eleven inserts derived from pCasJW1 completely rescued the dominant flightless behavior of *Ifm(3)99Eb*$^{E38}$ heterozygotes (Table I).

In addition to conferring dominant flightless behavior, *Ifm(3)99Eb*$^{E38}$ exhibits a recessive lethal phenotype. The ability of a transformed copy of the wild-type MLC-2 gene to rescue this recessive lethality was assayed as outlined in Fig. 1. Three inserts derived from pCasJW3 all rescue the recessive lethality of *Ifm(3)99Eb*$^{E38}$, and eight of 10 inserts derived from pCasJW1 rescue the recessive lethality of *Ifm(3)99Eb*$^{E38}$ to varying degrees, from 12 to 100% (Table I). From these results it is clear that the introduction of a transformed copy of the wild-type MLC-2 gene completely rescues the dominant flightless behavior and recessive lethality conferred by *Ifm(3)99Eb*$^{E38}$, confirming that *Ifm(3)99Eb* corresponds to the MLC-2 gene. Therefore, the *Ifm(3)99Eb* complementation group will be referred to hereafter as *Mlc2* and the *Ifm(3)99Eb*$^{E38}$ allele will be referred to as *Mlc2*$^{E38}$.

### *Mlc2*$^{E38}$ *Molecular Defect*

To determine the molecular defect responsible for the *Mlc2*$^{E38}$ mutation, we first examined genomic DNA from the *Mlc2*$^{E38}$ allele by Southern analysis to detect gross DNA rearrangements. No DNA rearrangement was found (data not shown; Warmke, 1990); however, this analysis identified a PstI restriction site polymorphism thereby simplifying the cloning of the *Mlc2*$^{E38}$ allele (see Materials and Methods). DNA sequencing revealed that the *Mlc2*$^{E38}$ allele contained 10 base pair changes within the MLC-2 transcription unit as compared to the wild-type Canton-S allele (data not shown; Warmke, 1990). The sequence of the MLC-2 gene obtained from a Canton-S chromosome was used for comparison, because the original *ca* stock used to generate the *Mlc2*$^{E38}$ mutation was not available. Therefore, we were not surprised

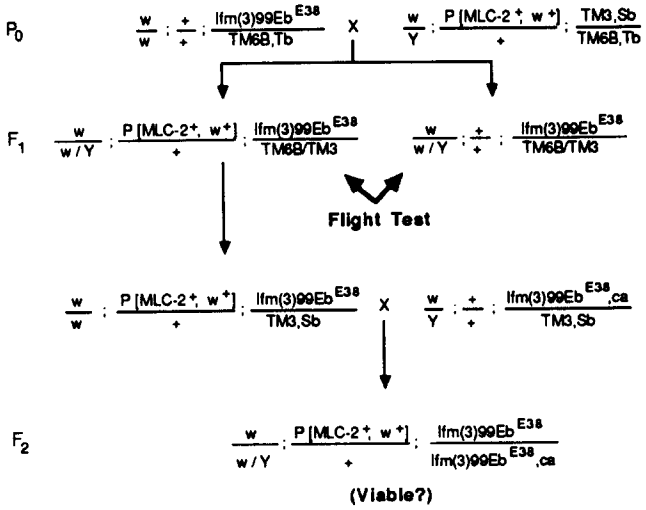


*Figure 1.* Crosses to rescue the dominant flightless behavior of *Ifm(3)99Eb*$^{E38}$ heterozygotes and the recessive lethality of *Ifm(3)99Eb*$^{E38}$. To determine if the dominant flightless behavior of *Ifm(3)99Eb*$^{E38}$ heterozygotes could be rescued by the introduction of a transformed copy of the wild-type MLC-2 gene (on the second chromosome), *w/w*; +/+; *Ifm(3)99Eb*$^{E38}$*/TM6B,Tb* virgin females were crossed with *w/Y; P[MLC-2*$^+$*w*$^+$*]/+ ; TM3,Sb/TM6B,Tb* males, where *P[MLC-2*$^+$ *w*$^+$*]* is a *P* element insertion containing wild-type copies of the MLC-2 and *white* genes from pCasJW1 or pCasJW3. $F_1$ progeny heterozygous for *Ifm(3)99Eb*$^{E38}$ and carrying (*w/w* or *Y; P[MLC-2*$^+$ *w*$^+$*]/+*; *Ifm(3)99Eb*$^{E38}$*/TM3,Sb* or *TM6B,Tb*) or lacking (*w/w* or *Y*; +/+; *Ifm(3)99Eb*$^{E38}$*/TM6B,Tb* or *TM3,Sb*) a transformed copy of the wild-type MLC-2 (*arrows*) were tested for flight ability. To determine if a wild-type copy of the MLC-2 gene could rescue the recessive lethality of *Ifm(3)99Eb*$^{E38}$, *w/w; P[MLC-2*$^+$ *w*$^+$*]/+*; *Ifm(3)99Eb*$^{E38}$*/TM3,Sb* virgin females were mated to *w/Y*; +/+; *Ifm(3)99Eb*$^{E38}$, *ca/TM3,Sb* males, and the percent of expected *w*$^+$, homozygous *Ifm(3)99Eb*$^{E38}$ progeny recovered was determined. If the wild-type copy of the MLC-2 gene rescues the recessive lethality of *Ifm(3)99Eb*$^{E38}$, then 25% of the viable progeny will be homozygous for *Ifm(3)99Eb*$^{E38}$.

to find as many as eight differences between the untranslated regions of the *Mlc2*$^{E38}$ and Canton-S alleles. More importantly, two base pair differences were identified within the translated sequences of the *Mlc2*$^{E38}$ and Canton-S alleles (Fig. 2). The first is an A to T transversion which results in an amber nonsense mutation at the 10th amino acid codon; and the second is an A to T transversion at the 13th amino acid codon, which results in a change from threonine to serine, but since this mutation is downstream of the nonsense mutation it is irrelevant in this case. Therefore, *Mlc2*$^{E38}$ is a null allele of the MLC-2 gene resulting from a nonsense mutation at the 10th codon.

### *MLC-2 Accumulation Is Reduced in Mlc2*$^{E38}$ *Heterozygotes*

Because *Mlc2*$^{E38}$ is a null mutation, we expected that expression of MLC-2 in *Mlc2*$^{E38}$ heterozygotes would be reduced by ~50% and that accumulation of MLC-2 protein would be reduced to a similar extent (O'Brien and MacIntyre, 1978). We have previously shown that MLC-2 RNA accumulation is reduced by ~50% in thoraces of *Mlc2*$^{E38}$ heterozygotes (Warmke et al., 1989). In the present study, we

*Table I. Summary of Ifm(3)99Eb$^{E38}$ Rescue Experiments*

| Line | Linkage group | Flight index‡ | Viability index§ |
|---|---|---|---|
| Canton-S | – | 7.4 ± 0.7 | – |
| *w; Ifm(3)99Eb$^{E38}$/TM6B,Tb* | – | 2.5 ± 2.2 | – |
| JW3-42.6 | *X* | 7.5 ± 0.8 | 73.6 |
| JW3-50.5 | *TM6,B,Tb* | 3.9 ± 3.0 | NA¶ |
| JW3-50.9 | *2* | 7.2 ± 1.0 | 97.4 |
| JW3-50.26 | *X* | 7.6 ± 0.6 | 90.0 |
| JW1-5.11 | *2* | 7.3 ± 0.8 | 88.6 |
| JW1-5.25 | *2* | 6.7 ± 1.7 | 65.1 |
| JW1-5.31 | *2* | 2.5 ± 2.7 | <1.8 |
| JW1-5.42 | *2* | 6.9 ± 1.4 | 42.0 |
| JW1-16.2 | *2* | 7.7 ± 0.5 | 55.1 |
| JW1-18.1 | *2* | 7.0 ± 0.9 | 40.0 |
| JW1-31.2 | *X* | 7.5 ± 0.6 | <3.3 |
| JW1-40.1 | *2* | 7.5 ± 0.7 | 71.3 |
| JW1-60.1* | *TM3,Sb* | 7.8 ± 0.4 | NA |
| JW1-62.5 | *2* | 7.2 ± 0.8 | 12.2 |
| JW1-63.1 | *2* | 7.6 ± 0.6 | 100.0 |

* A balanced rescued stock, denoted JW60, was constructed using this insert: *w; Ifm(3)99Eb$^{E38}$/TM3,Sb,P[w$^+$ MLC-2$^+$]*.
‡ A flight index of 0 indicates that the adults are incapable of flying or gliding; whereas, a flight index greater than 7 indicates that the adults are fully competent for flight. Intermediate flight indices indicate that the individuals have impaired flight ability; they may not be able to gain altitude, but they can glide. The flight indices for Canton-S and *w; Ifm(3)99Eb$^{E38}$/TM6B,Tb* adults is given followed by the results of the rescue experiments. For each transformed line, the flight index is of an *Ifm(3)99Eb$^{E38}$* heterozygotes carrying one copy of the transformed MLC-2 gene, *w; P[w$^+$ MLC-2$^+$]/+; Ifm(3)99Eb$^{E38}$/TM3,Sb* or *TM6B,Tb*.
§ The viability index is the percentage of expected *w; P[w$^+$ MLC-2$^+$]/+; Ifm(3)99Eb$^{E38}$/Ifm(3)99Eb$^{E38}$,ca* progeny recovered.
¶ Not applicable, because these inserts are on third chromosome balancers, they could not be introduced into a homozygous *Ifm(3)99Eb$^{E38}$* genetic background.

used Triton X-100–treated (skinned) IFM fibers to assay contraction kinetics at the single fiber level; therefore, we measured the MLC-2 content in single skinned IFM fibers representative of those used in subsequent functional assays. Inevitably, some proteins diffuse out of the fiber during the skinning procedures. Proteins that diffuse readily include glycolytic enzymes (Fig. 3 *a*, lane *2*), and those that diffuse out only after detergent treatment are primarily mitochondrial proteins (Fig. 3 *a*, lane *3*) (D. Maughan and J. Hurley, unpublished results). Immunoblots confirm that MLC-2 is not among the diffusible proteins in either wild type, *Mlc2$^{E38}$* heterozygotes, or a representative rescued line (Fig. 3 *b*, lanes *2–4, 6–8,* and *10–12*, respectively); rather, MLC-2 is confined solely to the cytomatrix (nondiffusible) fraction

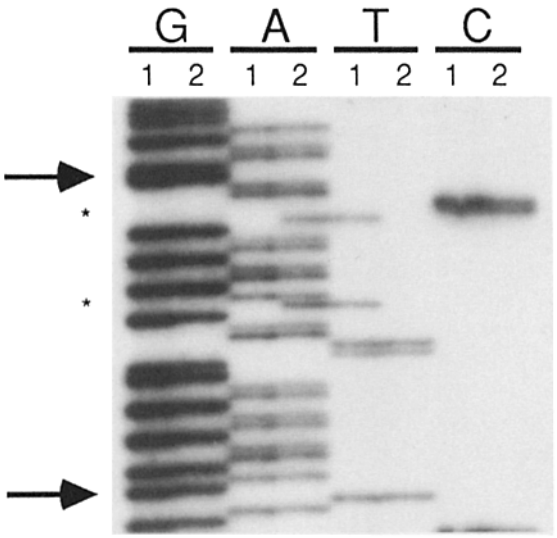


```
                4                                  10
                Glu Lys Lys Lys Val Lys Lys Lys Lys Thr Lys
Canton-S:       GAG AAG AAG AAG GTT AAG AAG AAG AAG ACC AAG

Mlc2 E38 :      --- --- --- --- --- --- T-- --- --- T-- ---
                Glu Lys Lys Lys Val Lys Stop
```

*Figure 2. Mlc2$^{E38}$* is a nonsense mutation at the tenth amino acid codon position. The sequencing reaction products from plasmids pBSTE-P/H2.2 (*Mlc2$^{E38}$*) and pBSTC-P/H2.2 (Canton-S) were loaded so that the *Mlc$^{E38}$* (1) and Canton-S (2) sequences could be compared directly. The asterisks (*) denote base differences. The DNA sequence between the arrows is given for Canton-S and *Mlc2$^{E38}$*, and the amino acid sequence for the wild-type Canton-S allele is presented above the corresponding DNA sequence, whereas the predicted amino acid sequence for the *Mlc2$^{E38}$* allele is given below the corresponding DNA sequence. Note that the A to T transversion in the tenth amino acid codon results in an amber nonsense mutation in the *Mlc2$^{E38}$* allele.

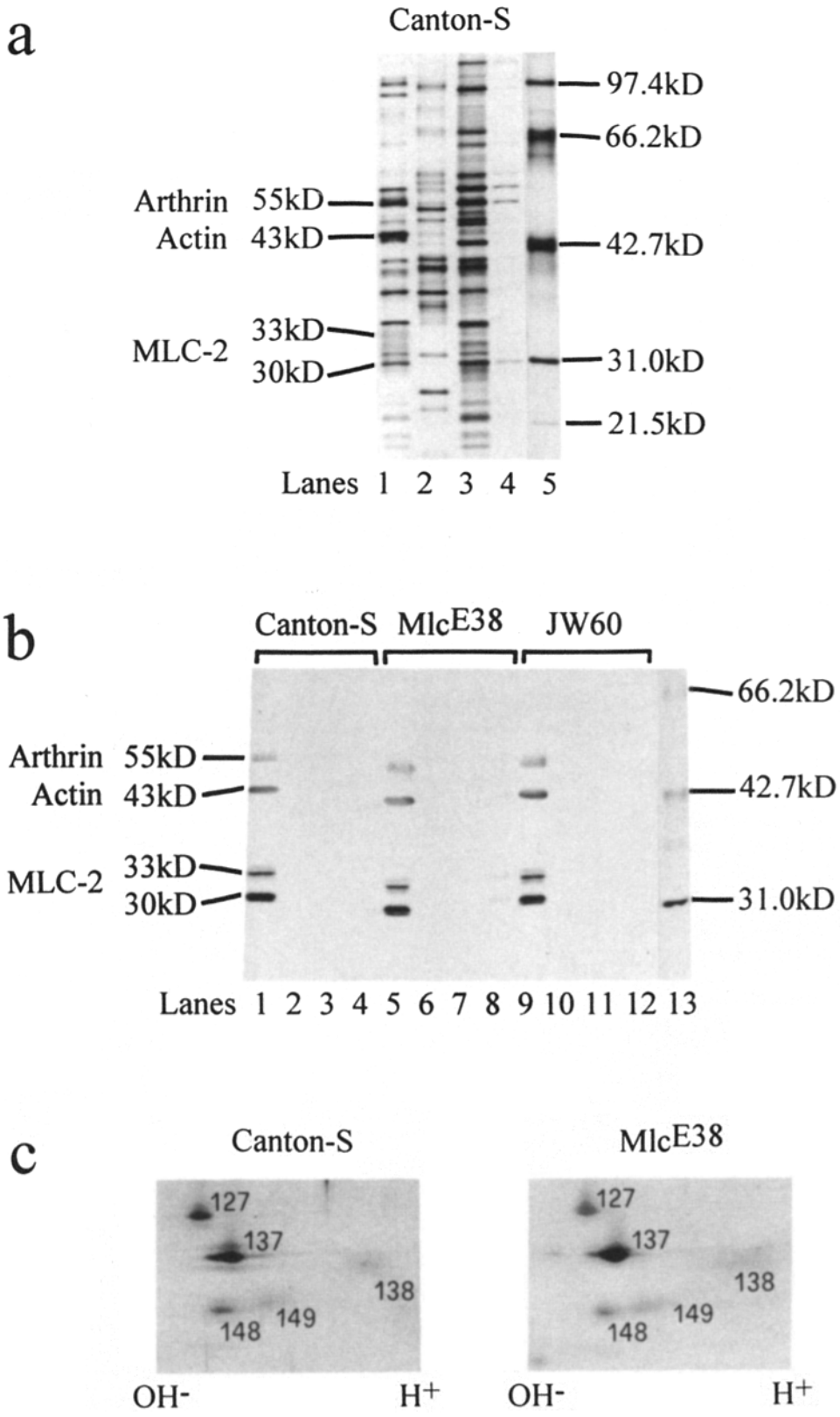


*Figure 3.* MLC-2 protein analysis of dorsal longitudinal indirect flight muscle of *Drosophila*. (*a*) Muscle fiber proteins separated by a diffusion method into three fractions: cytomatrix (lane *1*), containing the myofibrillar proteins; cytosol (lane *2*), containing readily diffusible proteins; and organelle (lane *3*), containing Triton X-100 extractable proteins (including those from mitochondria and sarcoplasmic reticulum). Lane *4* contains the combined rinses after the two extraction treatments. Protein samples were analyzed by electrophoresis using a 15% polyacrylamide slab gel, and the protein bands were silver stained. On this gel, 7% of the matrix (lane *1*), 10% of the cytosol (lane *2*), and 21% of the organelle (lane *3*) was loaded. All of the proteins in the combined rinse were loaded in lane *4*. Lane *5* contains molecular weight markers (Bio-Rad 161-0303 and 161-0304); molecular weights are indicated (in kD). (*b*) Immunoblot of IFM proteins reacted with rabbit anti-*Drosophila* MLC-2 and rat anti-actin sera. Samples from Canton-S (lanes *1–4*), $Mlc2^{E38}$ heterozygotes (lanes *5–8*), and JW60 (lanes *9–12*) were run on a 15% SDS-polyacrylamide gel and transferred to a nitrocellulose membrane for immune detection. Lanes *1*, *5*, and *9*, cytomatrix; lanes *2*, *6*, and *10*, cytosol; lanes *3*, *7*, and *11*, organelle; lanes *4*, *8*, and *12*, combined rinses after the two extraction treatments. Note the absence of MLC-2 and actin in cytosol and organelle fractions. 18% of the matrix in lane *1*, 23% of the matrix in lane *5*, and 22% of the matrix in lane *9* was loaded (the difference in MLC-2 concentration between these samples is not evident because the amount of MLC-2 in each sample is outside of the linear range of the HRP color development system). All other fractions were loaded at 100%. Lane *13* contains biotinylated standards (Bio-Rad 161-0306); molecular weights are indicated (in kD). (*c*) Cytomatrix proteins displayed on a two-dimensional gel (silver-stained). *Left*, Canton-S; *right*, $Mlc2^{E38}$ heterozygote. Proteins were separated in the first dimension using ampholines of pH 5–7; in the second dimension, by SDS-PAGE (12%). Protein identification is according to the convention of Mogami et al. (1982). Spot 148 is unphosphorylated MLC-2, spot 149 is phosphorylated MLC-2, and spot 138 appears to be a MLC-2 isoform that is phosphorylated and is posttranslationally modified (M. Graham, R. Tohtong, M. Chun and S. Falkenthal, manuscript in preparation). In this example, densitometry of spots 138, 148, and 149 indicates that MLC-2 accumulation in the IFM fiber from this $Mlc2^{E38}$ heterozygote is ~70% of that in Canton-S, taking into account differences in sample size (in this case, the $Mlc2^{E38}$ loading is ~10% greater than that of Canton-S as determined by normalization to the actin concentration); on average MLC-2 accumulation in $Mlc2^{E38}$ heterozygotes is ~59% of that in Canton-S ($n = 6$).

(lower two bands in Fig. 3 *b*, lanes *1*, *5*, and *9*, respectively), as are actin and arthrin, a unbiquinated form of actin (upper two bands in the same lanes). Note that the silver-stained gel (Fig. 3 *a*) shows a prominent protein band (at ~31 kD) within the pair of bands corresponding to MLC-2 (at 30 and 33 kD). The presence of this and possibly other overlapping bands precluded quantification of MLC-2 on the basis of silver stained one-dimensional gels.

In the present study, single IFM fibers were analyzed by two-dimensional electrophoresis to quantitate MLC-2 expression. Previous immunoblot analysis of two-dimensional gels of whole fly thoraces indicated that spots 138, 148, and 149 (nomenclature of Mogami et al., 1982) are different forms of MLC-2. These spots are easily resolved from the other proteins of the muscle fiber, and they all share common epitopes recognized by a rat anti-*Drosophila* MLC-2 antibody (M. Graham, R. Tohtong, M. Chun, and S. Falkenthal, in preparation). The amount of MLC-2 in each fiber was normalized to that of actin to correct for differences in fiber size. The densities of MLC-2 spots 138, 148, and 149 were summed (Fig. 3 *c*), and that sum divided by the sum of the spot densities of actin (spots 100 and 101). Fibers from $Mlc2^{E38}$ heterozygotes contained 0.59 ± 0.25 (mean ± SD, $n = 6$) of the amount of MLC-2 present in Canton-S (wild-type) fibers and 0.69 ± 0.16 ($n = 6$) of the amount of MLC-2 present in a balanced rescued line, JW60 (see Table I for a description of the JW60 line).

### *Development of the IFM Is Aberrant in $Mlc2^{E38}$ Heterozygotes*

To characterize the effect of reduced MLC-2 synthesis on IFM ultrastructure and assembly, we compared electron micrographs of intact IFM myofibrils from $Mlc2^{E38}$ heterozygotes and Canton-S (Figs. 4 and 5). Longitudinal sections (Fig. 4) showed that the average sarcomere length in $Mlc2^{E38}$ heterozygotes (3.6 ± 0.2 μm, $n = 25$) was about the same as that of wild type (3.5 ± 0.1 μm, $n = 25$). In contrast, myofibrils from $Mlc2^{E38}$ heterozygotes appear swollen due to altered thick and thin filament packing. Most noticeably, filaments peel away from the periphery of the myofibril (*large arrows*, Fig. 4 *b* and *c*), frequently entering an adjacent myofibril. Z lines are not as straight as in wild type but appear wavy and are sometimes broken (*small arrows*, Fig. 4 *b*).

Also evident in cross-section is the aberrant spacing of thick and thin filaments at the periphery of the myofibrils from $Mlc2^{E38}$ heterozygotes (Fig. 5 *b*). Although the arrangement and stoichiometry of six thin filaments surrounding one thick filament is reasonably well preserved (Fig. 5 *b*, *inset*), thin and thick filaments at the periphery of the myofibril do not appear to be as tightly associated with each other as in wild type myofibrils. In particular, a loss of tight double hexagonal packing can be seen as gaps between bundles of myofilaments within the myofibril (*arrows*, Fig. 5 *b*).

We also examined the ultrastructure of intact IFM myofibrils from pupae heterozygous for $Mlc2^{E38}$. Longitudinal sections and cross-sections of myofibrils from stage P14 pupae exhibited the same abnormalities as those described above for adult $Mlc2^{E38}$ heterozygotes; that is, the ultrastructural defects observed in heterozygous $Mlc2^{E38}$ adults and pupae were indistinguishable (data not shown; Warmke, 1990).

The aberrant spacing and alignment of peripheral lattice filaments in $Mlc2^{E38}$ heterozygotes is seen clearly in electron micrographs of skinned IFM fibers from 3–5-day-old adults prepared for mechanical and biochemical studies (Fig. 6 *d*). Also apparent is a striking reduction in the number of thick filaments in myofibrils from skinned fibers prepared in relaxing solution containing Triton X-100 as compared to the number of intact fibers (compare Fig. 5 *b* with Fig. 6 *c* and *d*): 357 ± 31 ($n = 16$) thick filaments per myofibril in skinned fibers versus 828 ± 93 ($n = 16$) thick filaments per myofibril in intact fibers from $Mlc2^{E38}$ heterozygotes. A concomitant reduction in the number of thin filaments is also observed. Apparently, about half the myofilaments slough off the myofibrils from $Mlc2^{E38}$ heterozygotes during extended (1–3 h) Triton X-100 treatment.

The number of myofilaments that slough off is sharply reduced if fibers from $Mlc2^{E38}$ heterozygotes are skinned while in rigor (ATP depleted) rather than while relaxed: 569 ± 85 ($n = 12$) thick filaments per myofibril versus 357 ± 31 ($n = 16$) thick filaments per myofibril, respectively. In fibers from wild type flies, thick filaments also appear to dissociate from the periphery of myofibrils during Triton X-100 treatment, but to a far lesser extent: in relaxing solution, 780 ± 46 ($n = 16$) thick filaments per myofibril in skinned fibers versus 861 ± 81 ($n = 16$) thick filaments per myofibril in intact fibers. These results suggest that the peripheral region of myofibrils from $Mlc2^{E38}$ heterozygote IFMs are considerably more susceptible to diffusional loss of myofilaments than the corresponding regions of wild-type muscle. Rigor crossbridges appear to stabilize the lattice structure in $Mlc2^{E38}$ heterozygotes, sharply reducing the diffusional loss of filaments from the peripheral regions of the myofibril presumably deficient in MLC-2.

Introducing a wild type copy of the MLC-2 gene rescues the IFM ultrastructural defects conferred by $Mlc2^{E38}$ (Figs. 4–6). The number of thick filaments per myofibril in intact flight muscle myofibrils from JW60 (881 ± 116, $n = 16$) is similar to that of Canton-S (861 ± 81, $n = 16$). Skinned muscle fibers from Canton-S and JW60, whether treated with Triton X-100 in relaxing or rigor solution, contain comparable numbers of thick filaments per myofibril to those in intact fibers. For example, in the skinned fibers shown in Fig. 6, the number of thick filaments per myofibril in Canton-S is 790 ± 14 ($n = 4$) and in JW60 is 993 ± 28 ($n = 4$).

### *$Mlc2^{E38}$ Confers Reduced Wing Beat Frequency and Flightless Behavior*

Flight in *Drosophila* is produced by the oscillatory contractions of the IFMs which deform the cuticle, thereby powering wing movement (Nachtigall and Wilson, 1967; Levine, 1973). The decrease in MLC-2 expression in $Mlc2^{E38}$ heterozygotes disrupts IFM function as indicated by reduced wing beat frequency and impaired flight ability. Table II summarizes measurements of wing beat frequencies and simple flight test results (see Materials and Methods) for Canton-S, $Mlc2^{E38}$ heterozygotes and JW60 conducted at 22 and 12°C. Canton-S and JW60 have similar wing beat frequencies, but $Mlc2^{E38}$ heterozygotes exhibit wing beat frequencies that are 30% (22°C) and 14% (12°C) less than those of Canton-S and JW60. Whereas, Canton-S and JW60 can fly at 22°C, $Mlc2^{E38}$ heterozygotes are flight impaired. Note that all three strains are flight impaired at 12°C and that the wing

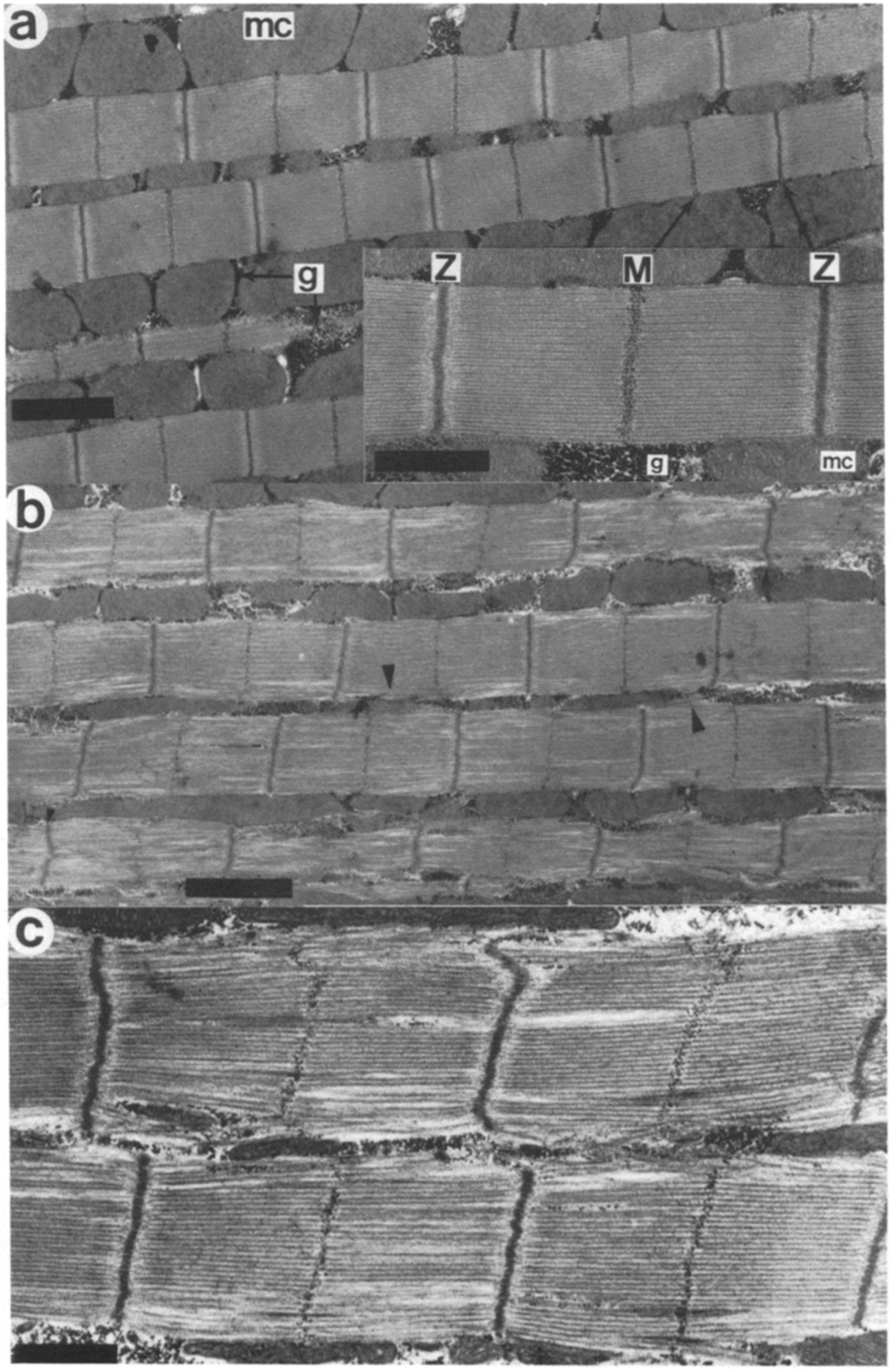
a
mc
g
Z
M
Z
g
mc
b
c

beat frequency at which *Mlc2*$^{E38}$ heterozygotes exhibits flight impairment at 22°C is close to that at which Canton-S and JW60 exhibit flight impairment at 12°C.

### *IFM Single Fiber Kinetics Are Altered by Reduced Mlc-2 Stoichiometry*

To investigate whether the reduced wing beat frequency conferred by *Mlc2*$^{E38}$ is associated with reduced contraction kinetics at the single fiber level, we compared mechanical and actomyosin ATPase rate constants in skinned single IFM fibers from Canton-S and *Mlc2*$^{E38}$ heterozygotes.

First, to establish the free $Ca^{2+}$ concentration at which activation of the skinned IFM fibers is maximal, ATPase rates were measured in skinned fibers held isometrically while immersed in ATP-salt solutions at various $Ca^{2+}$ concentrations. The free $Ca^{2+}$ concentration required for half maximal activation (~pCa 6) was similar in Canton-S and *Mlc2*$^{E38}$ heterozygotes (Fig. 7). Actomyosin ATPase activities of the fully activated isometrically held skinned IFM fibers of *Mlc2*$^{E38}$ heterozygotes were not significantly different from those of Canton-S (Table III). Maximal steady state active tension levels of the isometrically held skinned fibers at pCa 4–5 varied considerably from fiber to fiber. The mean tension level of *Mlc2*$^{E38}$ heterozygotes was 25% lower than that of Canton-S (Table III); however, the observed difference was not statistically significant ($P > 0.3$).

We next investigated the kinetic properties of the skinned fibers by measuring changes in force produced by the fibers in response to sinusoidal length perturbations. In particular, we focused on that part of the active response that corresponds to the phenomenon of stretch induced delayed tension rise, generally referred to as "stretch activation." Stretch activation, common to many types of muscle, is responsible for powering the oscillatory wing movement in insects (Jewell and Ruegg, 1966; Pringle, 1978). This effect can be studied by examining force responses to sinusoidal length perturbations (oscillatory changes in fiber length) applied at different frequencies (Kawai and Brandt, 1980; Thorson and White, 1983). A useful parameter that combines both force and length information is muscle stiffness. Muscle stiffness, the resistance of a muscle to stretch, is defined as the value of muscle force divided by the change in muscle length. Muscle stiffness can be converted into an intrinsic property (a stiffness modulus) by dividing the force changes by the cross-sectional area of the fiber and by dividing the length changes by the initial length of the fiber. For sinusoidal length changes, a convenient, concise format for presenting the stiffness data over a broad range of frequencies is the Nyquist plot (Kawai and Brandt, 1980). In a Nyquist plot (Fig. 8), the "elastic" stiffness modulus, corresponding to the component of force response in phase with the applied sinusoidal length change, is plotted along the $x$ axis. The magnitude of the elastic stiffness modulus reflects the number of attached crossbridges. The "viscous" stiffness modulus, corresponding to the component of force response that is 90° out-of-phase with the applied length change (delayed tension), is plotted along the $y$ axis. The negative viscous modulus represents that component of muscle stiffness that relates to actomyosin crossbridge cycling.

Nyquist plots for skinned fibers from Canton-S, *Mlc2*$^{E38}$ heterozygotes and JW60 in relaxed, active, and rigor states are shown in Fig. 8. The relaxed state corresponds to quiescent muscle (low $Ca^{2+}$, high ATP). The active state corresponds to contracting muscle (high $Ca^{2+}$, high ATP), whereas the rigor state corresponds to the muscle in rigor (ATP depleted). An active, force-generating fiber exhibits a marked increase (more negative) in viscous stiffness compared to its relaxed or rigor state, indicating that the skinned muscle fiber is performing mechanical work on the apparatus driving the oscillatory length changes. In addition, an active or rigor fiber has a higher elastic stiffness than in the relaxed state. Rigor stiffness is higher than active stiffness, indicating that more cross-bridges are attached in rigor than during active contraction.

The frequency at which the lowest (largest negative) viscous stiffness modulus occurs is a measure of the rate at which the process responsible for driving the wing beat occurs in vivo. This frequency (the so-called "bottom" frequency) is also the frequency at which maximum work is performed. The bottom frequency of skinned IFM fibers from *Mlc2*$^{E38}$ heterozygotes is ~15% lower than that of Canton-S (Table III); this reduction is significant at $P$ of 0.5. Rescue of *Mlc2*$^{E38}$ heterozygotes restores this frequency back to a value near that of Canton-S (Fig. 8 *c*).

## *Discussion*

We previously reported the molecular and genetic analysis of the 99D3 to 99E2-3 interval of the third chromosome and the identification of a putative MLC-2 mutation, *Ifm(3)99Eb*$^{E38}$ (Warmke et al., 1989). In this paper, we have used P element mediated germ line transformation and DNA sequence analysis to show that *Ifm(3)99Eb*$^{E38}$ is indeed a MLC-2 mutation. DNA sequence analysis revealed that the *Ifm(3)99Eb*$^{E38}$ mutation is an A to T transversion, which results in a nonsense mutation at the tenth codon of the MLC-2

*Figure 4.* Ultrastructure of the IFM of Canton-S and *Mlc2*$^{E38}$ heterozygotes. (*a*) Longitudinal section of wild type Canton-S IFM shows that the myofibrils are surrounded by many large mitochondria (*mc*) and collections of glycogen granules (*g*). The average sarcomeric length is 3.5 + 0.1 μm ($n$ = 25). The inset shows an enlargement of a representative sarcomere. The Z lines (*Z*) are the most electron dense structure of the sarcomere appearing very straight and compact. The M lines (*M*) are straight and well defined showing electron dense material (glycogen particles) distributed along the entire width of the sarcomere. Bars, (*a*) 2 μm; (*a, inset*) 1 μm. (*b*) Longitudinal section of the IFM from a *Mlc2*$^{E38}$ heterozygote demonstrates that the average sarcomere length of 3.6 ± 0.2 μm ($n$ = 25) is approximately the same as wild type. However, the M lines are not straight and are poorly defined at the periphery of the sarcomere. The Z lines are not as straight as in wild type but appear wavy and are sometimes broken (*small arrows*). The myofibrils appear swollen due to altered spatial arrangement of thick and thin filaments; filaments peel away from the periphery of the myofibril, and thick and thin filaments at the periphery of the myofibril form connections between adjacent myofibrils (*large arrows*). Bar, 2 μm. (*c*) A higher magnification view of a longitudinal section of the IFM from a *Mlc2*$^{E38}$ heterozygote showing that thick and thin filaments are exchanged between adjacent myofibrils. Bar, 1 μm.

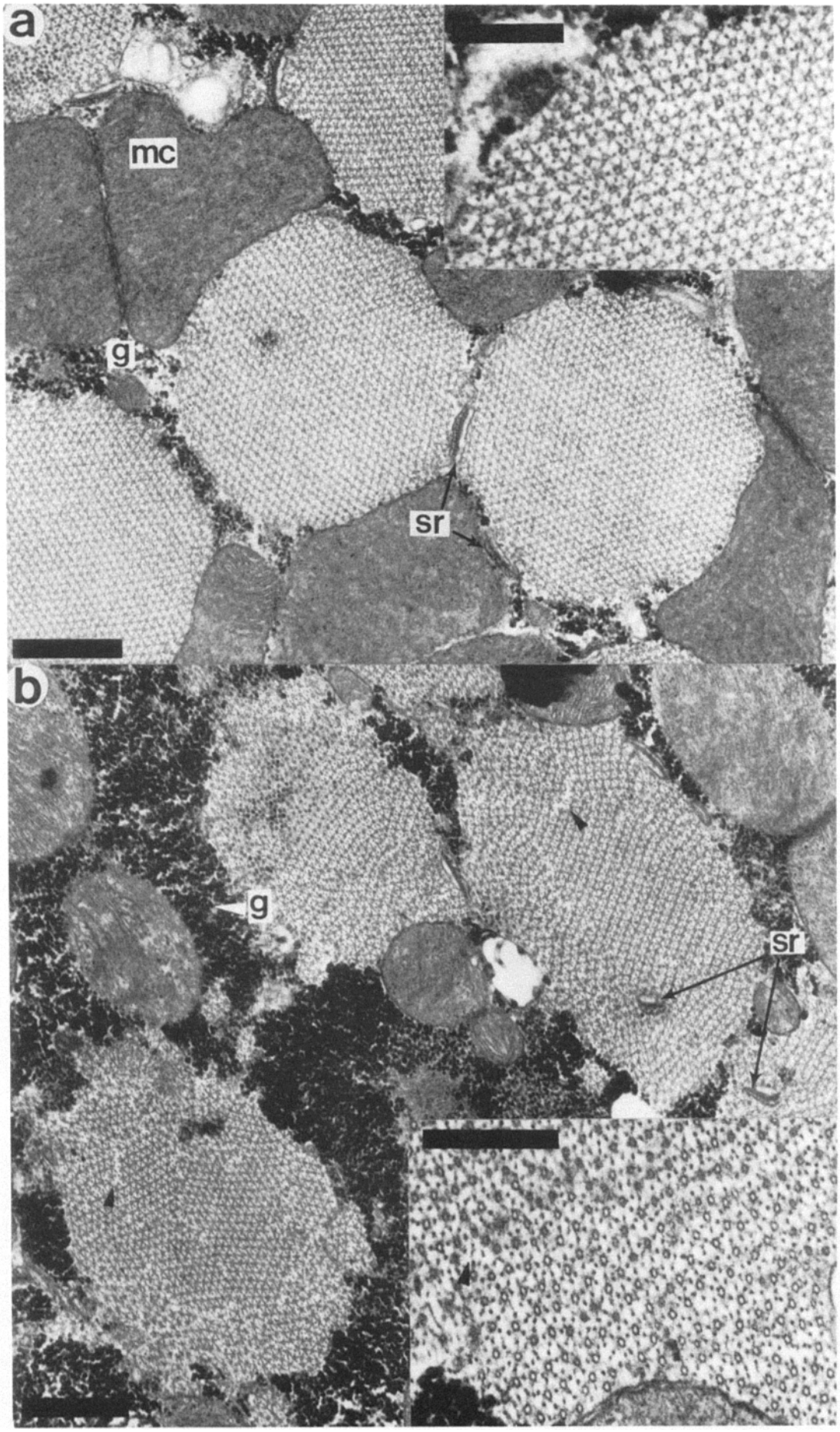
a
mc
g
sr
b
g
sr

gene. Therefore, *Ifm(3)99Eb*$^{E38}$ is a null mutation of the MLC-2 gene (*Mlc2*), and we have renamed the *Ifm(3)99Eb*$^{E38}$ allele to *Mlc2*$^{E38}$.

### *MLC-2 Is Essential for Viability*

The MLC-2 gene encodes a single protein isoform that is expressed in all muscle types throughout development (Parker et al., 1985; Toffenetti et al., 1987). Our initial genetic screen for MLC-2 mutations was based on the assumption that the MLC-2 gene is required for viability because it encodes the only sarcomeric MLC-2 isoform. *Mlc2*$^{E38}$ confers a recessive lethal phenotype which is rescued by the introduction of a wild type copy of the MLC-2 gene, thereby proving that expression of the MLC-2 gene is essential for viability. The lethal period for animals which lack MLC-2 is at the embryo-first instar larval boundary; that is, these embryos appear to undergo somewhat normal embryonic development but fail to hatch (data not shown; Warmke, 1990). Gastrulation, germ band extension and germ band shortening must be normal in homozygous *Mlc2*$^{E38}$ embryos because the cuticle of these embryos is wild type. Therefore, we propose that it is aberrant differentiation of the embryonic musculature in *Mlc2*$^{E38}$ homozygotes, a relatively late event in embryogenesis, that is responsible for their embryonic lethal phenotype. Analysis of the body wall muscles of homozygous *Mlc2*$^{E38}$ embryos will provide the unique opportunity to analyze myofibrillar assembly in vivo in the complete absence of MLC-2.

### *IFM Myofibrillar Assembly Requires Diploid Levels of MLC-2 Gene Expression*

The expression of MLC-2 in the IFM is gene dosage dependent. The relative amount of MLC-2 in single IFM fibers from *Mlc2*$^{E38}$ heterozygotes, expressed as a ratio of MLC-2 to actin content, is 59% of that in wild type. After Triton X-100 treatment in relaxing solution, approximately half the peripheral myofibrillar filaments slough off the myofibrils from *Mlc2*$^{E38}$ heterozygotes (Fig. 6). It is possible that these dissociated filaments lack (or have sharply reduced levels of) MLC-2. Immunoblots of triton X-100–treated skinned fibers showed little or no evidence of MLC-2 in the extracted protein fractions or wash solutions (Fig. 3 *b*). However, the absence of actin in these extracted fractions, strongly suggests that the dissociated filaments remain in the interfibrillar spaces vacated by the solubilized mitochondria (and thus remain effectively part of the cytomatrix fraction).

Electron microscopic studies of the differentiation of IFM myofibrils in *Drosophila* by Schafiq (1963) have revealed that early in myogenesis thick and thin filaments assemble into myofibrils composed of ~30 thick filaments each surrounded by six thin filaments in the normal double hexagonal array. As development proceeds, the myofibrils grow in both diameter and length. The length of the myofibrils is increased by an increase in sarcomere length, whereas the increase in myofibrillar diameter is due to the addition of Z disc material, thick filaments, and thin filaments at the periphery of the myofibril (Shafiq, 1963; Crossley, 1978; Sanger et al., 1986). Thick filament assembly is independent of thin filament assembly; however, the assembly of both filament systems is required for the proper alignment and registry of Z bands (Mahaffey et al., 1985; Chun and Falkenthal, 1988; O'Donnell and Bernstein, 1988; Beall et al., 1989). It has been proposed that the interaction of thick and thin filaments via the myosin cross-bridge is responsible for the correct registration of the sarcomeres (O'Donnell and Bernstein, 1988; Beall et al., 1989). If so, a mutation that alters the ratio of thick to thin filaments or affects cross-bridge formation would also be expected to cause aberrant myofibrillar assembly. As expected, mutations in the genes encoding myosin heavy chain, troponin T and the IFM specific isoform of actin have been shown to result in aberrant myofibrillar assembly in heterozygotes (Mogami et al., 1981; Mahaffey et al., 1985; Chun and Falkenthal, 1988; O'Donnell and Bernstein, 1988; Beall et al., 1989; Fyrberg et al., 1990). Electron microscopy of IFMs from heterozygous troponin T and actin null mutants revealed that these mutations reduced the number of thin filaments by ~50%, whereas heterozygous myosin heavy chain null mutants exhibit an ~50% reduction in the number of thick filaments. The common ultrastructural defect conferred by these myofibrillar protein deficiencies is that the central core of the myofibril appears to assemble normally; however, the arrangement of myofilaments at the periphery of the myofibrils is aberrant due to the altered ratio of thick to thin filaments (Mogami et al., 1981; Chun and Falkenthal, 1988; Beall et al., 1989).

We have shown that the number of thick filaments is not reduced in the IFM of *Mlc2*$^{E38}$ heterozygotes. What could cause the observed disruption of myofibrillar structure in the IFM of *Mlc2*$^{E38}$ heterozygotes in which the ratio of thick to thin filaments is unaltered? The most likely causes are either that (*1*) the thick and thin filaments fail to associate in the proper hexagonal packing during myogenesis, or that (*2*) the proper hexagonal packing of the thick and thin filaments is disrupted during the initial contractions of the IFM following eclosion. The IFM do not contract until several hours post-eclosion (Takahashi et al., 1990); consequently, we examined the IFM of stage P14 heterozygous *Mlc2*$^{E38}$ pupae to determine if the thick and thin filaments assemble into their

*Figure 5.* Ultrastructure of the IFM of Canton-S and *Mlc2*$^{E38}$ heterozygotes. (*a*) As seen in cross-section, wild-type Canton-S IFM myofibrils are cylindrical and are surrounded by many large mitochondria (*mc*) and collections of glycogen granules (*g*). Elements of the sarcoplasmic reticulum (*sr*) are visible around the exterior of the myofibrils. Within each myofibril, the myofilaments are arranged in a rigid double hexagonal array. (*a, inset*) Six thin filaments surround each thick filament, and the thick filaments are also arranged in a regular hexagonal array. Bars, (*a*) 0.5 μm; (*a, inset*) 0.25 μm. (*b*) Cross-section of a myofiber from a *Mlc2*$^{E38}$ heterozygote reveals that the cylindrical aspect of the myofibrils is lost. Thick filaments and surrounding thin filaments are found randomly positioned instead of in tight hexagonal packing at the periphery of the myofibril (*b, inset*). Large gaps appear between bundles of myofilaments (*arrows*). Elements of the sarcoplasmic reticulum (*sr*) are found within the interior of the myofibril. (*b, inset*) The ordered double hexagonal packing of the thick and thin filaments at the periphery of the myofibril is disrupted, and gaps where thick filaments are missing can be seen (*arrow*). Bars, (*b*) 0.5 μm; (*b, inset*) 0.25 μm.

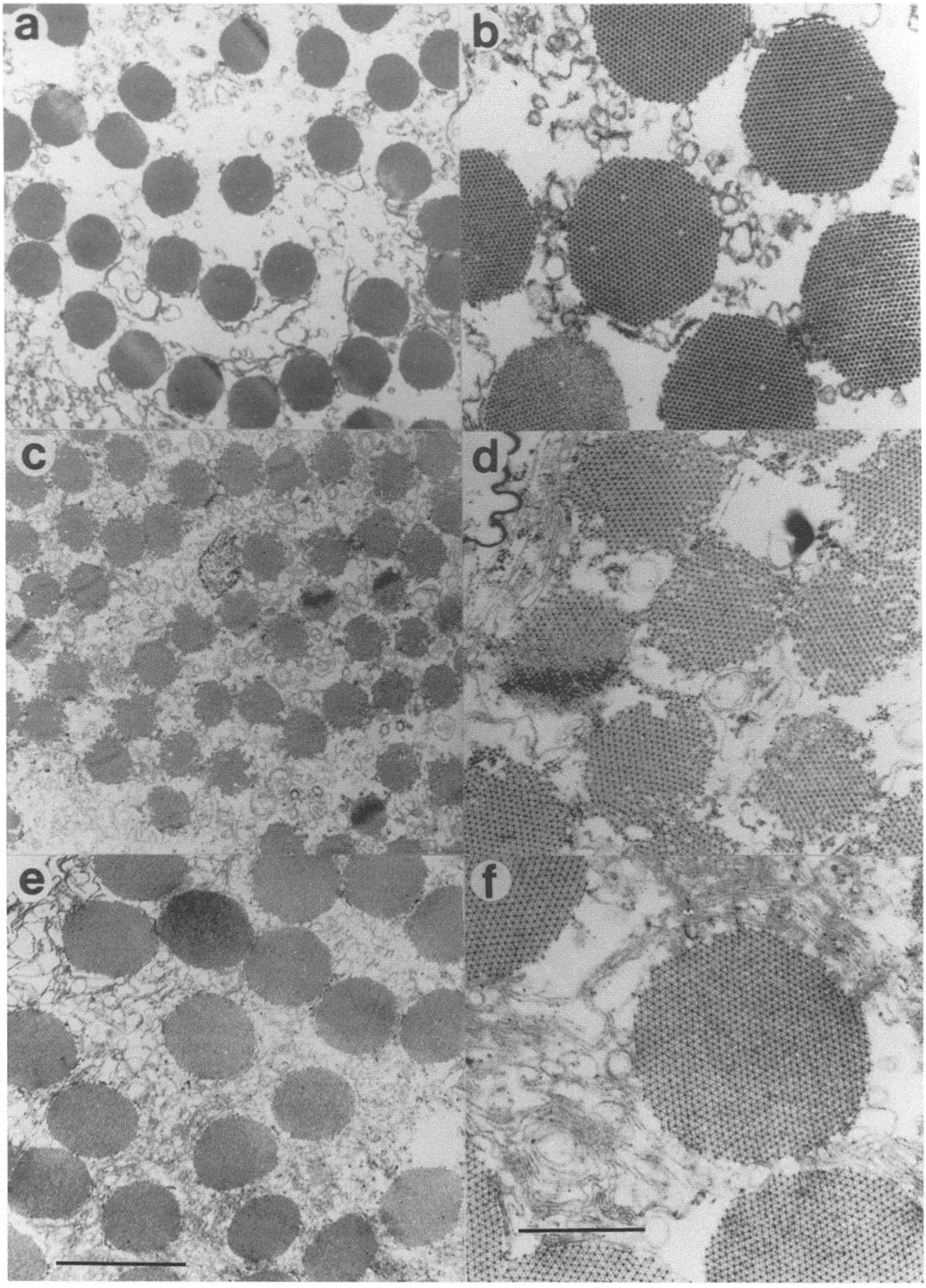
a
b
c
d
e
f

*Table II. Flight and Wing Beat Frequency Analysis*

| Line | Flight Score* 22°C | Flight Score* 12°C | Wing Beat Frequency§ 22°C | Wing Beat Frequency§ 12°C |
|---|---|---|---|---|
| Canton-S | U | D | 218 ± 19 (5)‡ | 145 ± 16 (6) |
| $Mlc2^{E38}$ heterozygotes | D | D | 149 ± 12 (4) | 124 ± 8 (3) |
| JW60 | U | D | 208 ± 16 (4) | 144 ± 22 (6) |

* U, flighted (gained elevation in flight at least once in 10 trials); D, flight impaired (did not gain elevation in flight in all ten trials).
‡ Number of flies tested.
§ In cycles per second (Hz).

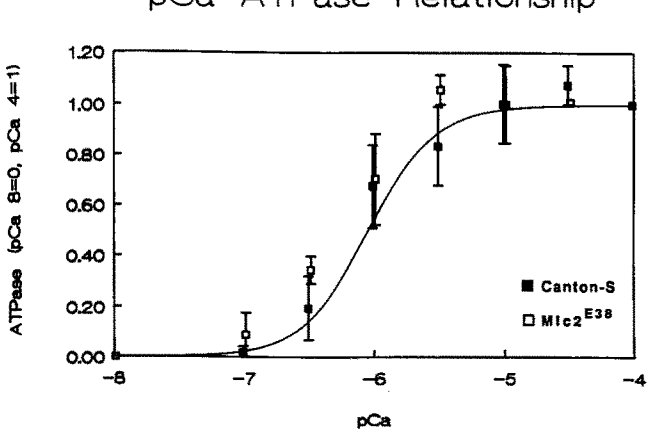


*Figure 7.* pCa-ATPase relationship in wild-type and $Mlc2^{E38}$ heterozygotes. Steady state ATPase rate versus calcium concentration in skinned IFM fibers from Canton-S (*filled squares*) and $Mlc2^{E38}$ heterozygotes (*open squares*). Means and standard deviations are indicated. The solid line is the best fit of the wild-type data to the Hill equation: ATPase = $[Ca^{2+}]^n/Ca^{2+}{}_{50} + [Ca^{2+}]^n$, where ATPase is relative to that at pCa 4, $Ca^{2+}{}_{50}$ is the calcium concentration giving 50% activation of ATPase (1 $\mu$M), and $n$ is the Hill coefficient (1.7). Note that the steady state ATPase activity of Canton-S and $Mlc2^{E38}$ heterozygotes exhibit similar calcium sensitivities. Temperature, 12°C.

proper hexagonal array during myogenesis. Analysis of longitudinal sections and cross-sections of the IFM of these pupae revealed that the myofibrils are indistinguishable from those of heterozygous $Mlc2^{E38}$ adults. Therefore, we conclude that the structural defects observed in the IFM of $Mlc2^{E38}$ heterozygotes result from the absence of some key structural role MLC-2 plays during myofilament lattice formation.

MLC-2 is associated with the globular head of the myosin heavy chain and is believed to modulate the actin-activated–myosin-linked $Mg^{2+}$-ATPase (Sweeney and Stull, 1990, and references therein). Because myosin molecules assembly into thick filaments via interactions between the rod portion of the myosin molecule, it is not surprising that a reduction in MLC-2 stoichiometry has no effect on thick filament assembly. However, MLC-2 has been implicated in stabilizing the neck region of the myosin molecule and in maintaining the ordered helical array of myosin heads on relaxed myosin filaments (Vibert and Craig, 1985). Furthermore, it has been proposed that MLC-2 may also play an important role in keeping the two heads of each individual myosin molecule apart from one another because myosin devoid of MLC-2 forms intermolecular aggregates with many myosin heads clumped together (Schaub et al., 1986). Therefore, if the ordered helical arrangement of each individual myosin head around the thick filament is responsible for establishing the regular hexagonal packing of six thin filaments around each thick filament during myofilament lattice formation, then the disordered arrangement of myosin heads due to the absence of MLC-2 would result in aberrant association of thick and thin filaments during sarcomere assembly.

Our results support the idea that the core of the myofibril is assembled early in myogenesis. During the initiation of myofibrillar assembly in $Mlc2^{E38}$ heterozygotes, it is likely that sufficient MLC-2 is synthesized from the single wild type copy of the MLC-2 gene to assemble myosin hexamers with the correct MLC-2/MHC stoichiometry, and this myosin forms the thick filaments at the core of the myofibrils. However, during later stages of myofibrillar assembly the available pool of MLC-2 becomes exhausted, resulting in thick filaments with little or no MLC-2, leading to lattice disorder at the periphery of the myofibril for reasons discussed above. A more complete understanding of how de-

*Table III. Mechanical, Biochemical, and Kinetic Properties of Skinned Muscle Fibers*

| Line | Active ATPase ($s^{-1}$)* | Maximum tension (kN $m^{-2}$) | Bottom frequency§ (Hz) |
|---|---|---|---|
| Canton-S | 1.9 ± 0.3 (7) | 2.88 ± 2.09 (8)‡ | 115.9 ± 14.1 (20) |
| $Mlc2^{E38}$ heterozygotes | 2.3 ± 0.7 (6) | 2.16 ± 1.56 (5) | 98.6 ± 18.4 (7)¶ |

Summary of steady-state mechanical and biochemical parameters in isometrically held, $Ca^{2+}$-activated skinned IFM fibers (maximum tension and active ATPase activity) and kinetics of force response to sinusoidal length changes in $Ca^{2+}$-activated IFM skinned fibers (bottom frequency) from Canton-S and $Mlc2^{E38}$ heterozygotes. Temperature, 10–14°C.
* Active ATPase = $ATPase_{(pCa\ 4)} - ATPase_{(pCa\ 8)}$; pmol ATP per pmol myosin subfragment 1 (S1) per second.
‡ Number of independent fibers analyzed.
§ Related to the rate of stretch activation.
¶ Significantly different at p of 0.05 using the $t$ test.

*Figure 6.* Cross-sections of isolated, Triton X-100–treated skinned single IFM fibers of Canton-S (*a* and *b*), $Mlc2^{E38}$ heterozygotes (*c* and *d*), and JW60 (*e* and *f*). The myofibrils are delineated clearly in these fibers that have been cleared of most mitochondria and sarcoplasmic reticulum by Triton X-100 treatment. Mitochondrial fragments remain, but there is no remaining glycogen granules or sarcoplasmic reticulum as seen in sections from intact fibers (Figs. *4* and *5*). In skinned fibers, there are fewer myofilaments in the myofibrils of MLC-2 deficient flies ($Mlc2^{E38}$ heterozygotes, 357 ± 31, $n$ = 16) than in wild-type flies (Canton-S, 780 ± 46, $n$ = 16) or in rescued flies (JW60, 993 ± 28, $n$ = 4). Bars, (*a*, *c*, and *e*) 3 $\mu$m; (*b*, *d*, and *f*) 1 $\mu$m.

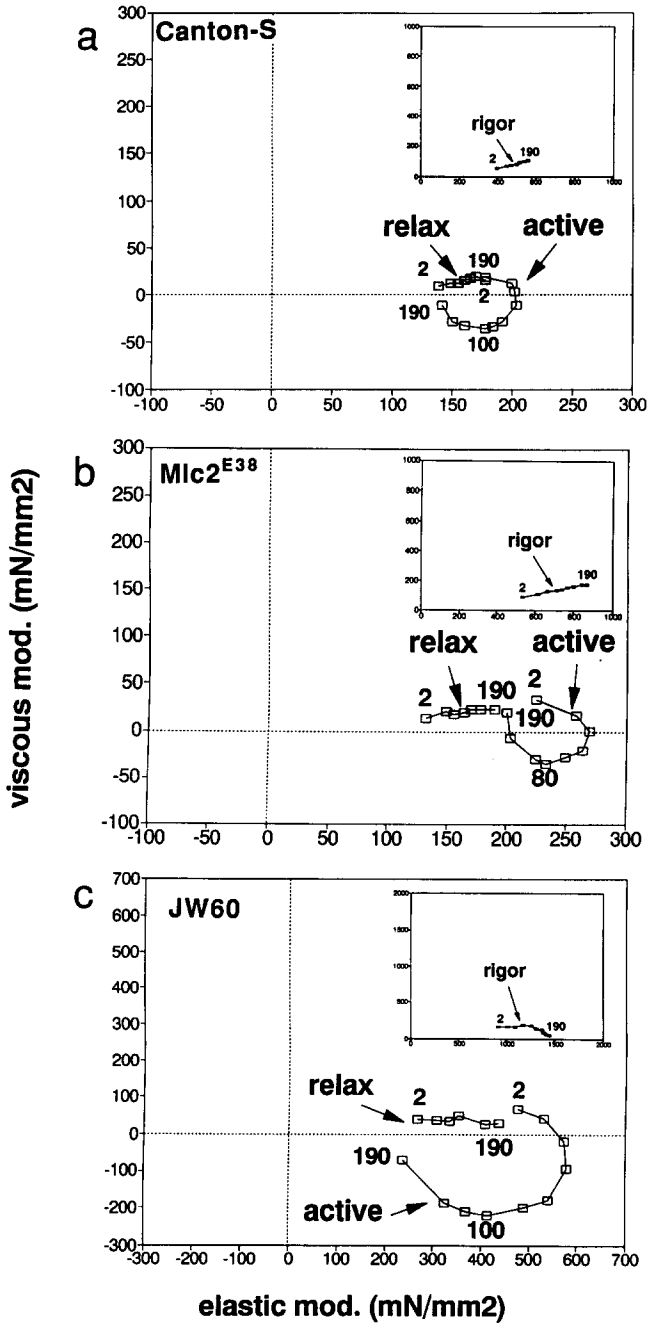


*Figure 8.* Nyquist plots of skinned IFM fibers in solutions producing relaxation (relax), $Ca^{2+}$ activation (active), and rigor. (*a*) Canton-S; (*b*) *Mlc2*$^{E38}$ heterozygotes; (*c*) JW60. In the Nyquist plot, the elastic stiffness modulus (*x*-axis), in phase with the applied sinusoidal length change, reflects the number of attached cross-bridges. The viscous stiffness modulus (*y*-axis), 90° out-of-phase with the applied sinusoidal length change of the same frequency, is believed to reflect that component of muscle stiffness that relates to actomyosin cross-bridge cycling. Frequencies used are indicated on the curves. The frequency at which the viscous stiffness modulus attains its largest negative value (the bottom frequency) is related to the wing beat frequency when compared at the same temperature. In this example, the bottom frequency of *Mlc2*$^{E38}$ heterozygotes (~80 $s^{-1}$) is ~20% less than that of Canton-S and JW60 (~100 $s^{-1}$). The specific values for the elastic stiffness modulus and the viscous stiffness modulus (at the same frequencies) varied considerably from fiber to fiber (within and between strains) due both to the large variability in muscle stiffness and tension between

creased expression of MLC-2 affects sarcomere structure requires quantitative immunofluorescence microscopy to determine the concentration of MLC-2 at the center and at the periphery of the myofibril.

### *Impaired Flight Behavior and Reduced Wing Beat Frequency Associated with Reduced MLC-2 Concentration*

IFM function in *Drosophila* is very sensitive to gene dosage. Hemizygosity of the sarcomeric myosin heavy chain gene (*Mhc36B*) and the *Act88F* gene (which encodes the IFM-specific actin isoform) both result in dominant flightless behavior (Mogami et al., 1986; Hiromi and Hotta, 1985; Mahaffey et al., 1985). Likewise, mutations that block the expression of troponin I, troponin T, and the IFM-specific tropomyosin isoform also exhibit dominant flightless behavior (Karlik and Fyrberg, 1985; Tansey et al., 1987; Fyrberg et al., 1990; Barbas et al., 1991; Beall and Fyrberg, 1991). *Mlc2*$^{E38}$ heterozygotes are also flight impaired (flight index 2.5 ± 2.2 for *Mlc2*$^{E38}$ heterozygotes and 7.4 ± 0.7 for Canton-S; Table I). The flight impaired *Mlc2*$^{E38}$ heterozygotes beat their wings at a frequency 30% lower than that of Canton-S. Flight is fully rescued in JW60 (flight index 7.8 ± 0.4) and wing beat frequency is similar to wild type (Table II).

Flight tests are used extensively to screen for mutants that may have structural changes in their IFMs due to a mutation in a sarcomeric protein. However, wing beat analysis may provide a quantitative link to characterize the underlying structural defect. Because wing beat frequency is related to the kinetics of the flight muscle (Molloy et al., 1987), we examined the properties of single IFM fibers, focusing on their contraction kinetics.

Single fiber kinetic experiments were carried out at 12°C to avoid any possibility of diffusion limitation of substrate (see Materials and Methods). Thus, wing beat frequency measurements and simple flight tests were repeated at 12°C in order to correlate these three sets of data at the same temperature. At 12°C, the wing beat frequency of *Mlc2*$^{E38}$ heterozygotes was ~15% less than Canton-S and JW60. This difference is less than the difference observed at 22°C (~30%).

At 12°C, both Canton-S and JW60 were flight impaired with wing beat frequencies (145 and 144 Hz, respectively) close to that of flight impaired *Mlc2*$^{E38}$ heterozygotes at 22°C (149 Hz). This result suggests that wing movements in the lower range of 145–149 Hz do not provide sufficient power for flight.

### *Relationship of Flightlessness, Wing Beat Frequency, and Viscoelastic Properties of the IFM Fiber*

The wing beat frequency of *Drosophila* is determined primarily by the load on the wings and the viscoelastic properties of the cuticle and flight muscle (Pringle, 1978). The wing beat frequency can be lowered by reducing the overall muscle fiber stiffness, which can be accomplished in three

fibers (Table III) and to the unavoidable differences in the compliance of the attachment points for each fiber; most importantly however, fibers from *Mlc2*$^{E38}$ heterozygotes consistently exhibited a statistically significant reduction (~15%, Table III) in bottom frequency as compared to Canton-S and JW60. Temperature, 12°C.

ways: by (*1*) reducing the total number of myofilaments in the fiber, (*2*) reducing the stiffness of each cross-bridge in the active fiber, or (*3*) reducing resting fiber stiffness resulting in a reduction in overall muscle fiber stiffness.

Possibility (*1*) can be directly tested. Myofibrils of intact muscle fibers from *Mlc2*$^{E38}$ heterozygotes have as many myofilaments as those from Canton-S (Fig. 5). The density of myofibrils in the fibers also appears to be nearly equivalent. Thus, reduced wing beat frequency in *Mlc2*$^{E38}$ heterozygotes is not due simply to a reduction in the number of filaments per muscle fiber.

Separate changes in active (possibility *2*) or resting (possibility *3*) muscle stiffness as a result of the MLC-2 deficiency cannot be excluded. Notably, intact IFM fibers from Canton-S and *Mlc2*$^{E38}$ heterozygotes have the same density of myofibrils. However, skinned fibers from *Mlc2*$^{E38}$ heterozygotes contain as few as half the number of thick filaments per myofibril as those of Canton-S and JW60. It is tempting to speculate that MLC-2 deficient peripheral regions of myofibrils of *Mlc2*$^{E38}$ heterozygotes are structurally unstable and therefore unable to support force generation, in contrast to the normal myofibrillar core remaining in the skinned fibers. If so, this would result in a reduction in the overall active muscle stiffness, thereby leading to a reduced wing beat frequency (Molloy et al., 1992).

The question arises why, in light of the ultrastructural differences, the functional properties of skinned fibers from *Mlc2*$^{E38}$ heterozygotes are not more markedly different from those of wild type flies. Steady active force tends to be lower in *Mlc2*$^{E38}$ heterozygotes (compare means for each strain in Table III); however, the standard deviations are large and the observed differences in steady active force and ATPase are not statistically significant. The well-organized core of myofibrils remaining in the detergent-treated skinned fibers of *Mlc2*$^{E38}$ heterozygotes contribute most to the fiber cross-sectional area to which force and ATPase are normalized. Thus, it is not surprising that skinned fibers from *Mlc2*$^{E38}$ heterozygotes exhibit near wild type properties, arising from the core portion of the myofilament lattice that probably possesses wild-type MLC-2/myosin heavy chain stoichiometry.

However, close examination of the contraction kinetics indicate differences in stretch activation that are likely attributable to myofibrillar regions with reduced MLC-2/myosin heavy chain stoichiometry that remain within the sarcomere after detergent treatment. Sinusoidal analysis of skinned IFM fibers allowed us to examine that portion of the force response (negative stiffness viscous modulus: Kawai and Brandt, 1980) responsible for mechanical work output (delayed tension). Sinusoidal analysis shows that the frequency at which maximum work is obtained (i.e., the "bottom" frequency) in the isolated fiber is ~15% lower in *Mlc2*$^{E38}$ heterozygotes than in Canton-S and JW60 at 12°C (Table III; Fig. 8). This 15% difference between the bottom frequency of Canton-S and *Mlc2*$^{E38}$ heterozygotes is within the range of differences reported (5–40%) in a preliminary study using pseudorandom white noise analysis (Yamakawa et al., 1991). Because wing beat frequency can also be lowered by reducing the bottom frequency and thus reducing the stiffness of the active muscle fiber, it is tempting to speculate that the reduced wing beat frequency of *Mlc2*$^{E38}$ heterozygotes ultimately derives from altered contraction kinetics of regions with no MLC-2 or with reduced MLC-2/myosin heavy chain ratio.

How could a deficiency of MLC-2 affect contraction kinetics? There are at least two possibilities: (*1*) At the molecular level, the presence of MLC-2 on the globular head of the myosin molecule may be required for optimum actomyosin interaction. In scallop myosin filaments, removal of the regulatory light chains (MLC-2) causes the helical arrangement of myosin heads to be disrupted (Vibert and Craig, 1985). If the light chains are responsible for maintaining the separation and orientation of the myosin heads that is optimum for interacting with actin (Schaub et al., 1986), then one would expect that in a MLC-2 deficient activated fiber the contraction kinetics would be slower. In fact, the kinetics of the force response to sinusoidal length perturbation have been shown to be correlated with the specific MLC-2 isoform in fast and slow muscle types in rabbit (Kawai and Schachat, 1984). Removal of one-third of the MLC-2 by chemical extraction has also been shown to produce a 50% reduction in unloaded shortening velocity (Moss et al., 1982). A small reduction in mean peak tension (0.78 $\pm$ 0.12 of that measured before the light chain extraction) was also reported. Our results are consistent with these previous findings; that is, the IFM of *Mlc2*$^{E38}$ heterozygotes, which exhibit a 40% reduction in MLC-2 accumulation, have slower contraction kinetics than wild type as indicated by the lower oscillation frequency at which maximum work output occurs (Table III). (*2*) At the level of the sarcomere, our results indicate that normal stoichiometry of MLC-2 is required for proper assembly of the myofilament lattice. It is possible that the observed changes in M and Z line structures (Figs. 4 and 5) reduce resting stiffness in *Mlc2*$^{E38}$ heterozygotes, thereby leading to a reduction in strain on the fiber. A reduction in stretch activation could be brought about by the reduced strain on a strain sensor in those peripheral filaments deficient in MLC-2. The strain sensor might be elastic connections between the thick filaments and the Z line (Auber and Couteaux, 1963; White, 1983; Nave and Weber, 1990) or troponin-H (Bullard et al., 1988).

Alternatively, sarcomeric disorder itself might reduce the rate of stretch activation. In asynchronous flight muscle, sarcomeric order (particularly the alignment of thick and thin filaments) appears to be critical for producing stretch activation (Wray, 1979; Tregear, 1983). Loss of thick and thin filament alignment in the peripheral regions of the myofibril may therefore contribute to reducing the overall rate of stretch activation.

## Conclusions

We have shown that *Mlc2*$^{E38}$ is a null mutation of the MLC-2 gene and results in reduced accumulation of MLC-2 protein in the IFM. The analysis of *Mlc2*$^{E38}$ heterozygotes reveals that wild-type MLC-2 stoichiometry is required for normal myofilament lattice alignment during IFM myogenesis and for normal IFM function as assayed by flight behavior, wing beat frequency and single fiber mechanics. These analyses confirm that the IFM of *Drosophila* is a useful system for analyzing MLC-2 function in vivo. Furthermore, because *Mlc2*$^{E38}$ is a null mutation and the ultrastructural and functional defects conferred by *Mlc2*$^{E38}$ can be completely rescued by P-element mediated germline transformation, the *Mlc2*$^{E38}$ allele provides an ideal genetic background for the analysis of MLC-2 mutations generated in vitro in future studies of MLC-2 structure and function in vivo.

We regret that Scott Falkenthal passed away during the preparation of this manuscript. We therefore dedicate this paper to his memory.

We thank Janet Hurley, Richard Schaaf, and Kevin Bickford for their assistance during the course of this work. We thank Melissa Graham for providing the anti-*Drosophila* MLC-2 sera. We also thank Miyoung Chun for her technical assistance and providing the electron micrographs of intact Canton-S IFM shown here.

We appreciate grant support for D. Maughan from the National Institutes of Health (R01 AR40234) and for S. Falkenthal from the National Institutes of Health (GM33270). J. E. Molloy was a visiting North Atlantic Treaty Organization (NATO) fellow.

Received for publication 17 December 1991 and in revised form 5 August 1992.

### *References*

Adelstein, R. S., and E. Eisenberg. 1980. Regulation and kinetics of the actin-myosin-ATP interaction. *Annu. Rev. Biochem.* 49:921–956.

Auber, J., and R. Couteaux. 1963. Ultrastructure de la striez dans des muscles de dipteres. *J. Microsc. (Paris).* 2:309–324.

Bainbridge, S. P., and M. Brownes. 1981. Staging the metamorphosis of *Drosophila melanogaster*. *J. Embryol. Exp. Morphol.* 66:57–80.

Barbas, J. A., J. Galceran, I. Krah-Jentgens, J. L. de la Pompa, I. Canal, O. Pongs, and A. Ferrus. 1991. Troponin I is encoded in the haplolethal region of the *Shaker* gene complex of *Drosophila*. *Genes Dev.* 5:132–140.

Beall, C. J., and E. Fyrberg. 1991. Muscle abnormalities in *Drosophila melanogaster heldup* mutants are caused by missing or aberrant troponin-I isoforms. *J. Cell Biol.* 114:941–951.

Beall, C. J., M. A. Sepanski, and E. A. Fyrberg. 1989. Genetic dissection of *Drosophila* myofibril formation: effects of actin and myosin heavy chain null alleles. *Genes Dev.* 3:131–140.

Benton, W. D., and R. W. Davis. 1978. Screening λgt recombinant clones by hybridization to single plaques in situ. *Science (Wash. DC).* 196:180–182.

Benzer, S. 1973. Genetic dissection of behavior. *Sci. Am.* 229:24–37.

Bullard, B., K. Leonard, A. Larkins, G. Butcher, C. Karlik, and E. Fyrberg. 1988. Troponin of asynchronous flight muscle. *J. Mol. Biol.* 204:621–637.

Chun, M., and S. Falkenthal. 1988. *Ifm(2)2* is a myosin heavy chain allele that disrupts myofibrillar assembly only in the indirect flight muscle of *Drosophila melanogaster*. *J. Cell Biol.* 107:2613–2621.

Craymer, L. 1984. Report. *Drosophila Inform. Serv.* 60:234–236.

Cross, R. L., and P. D. Boyer. 1975. The rapid labelling of adenosine triphosphate by $^{32}$P-labelled inorganic phosphate and the exchange of phosphate oxygens as related to conformational coupling in oxidative phosphorylation. *Biochemistry.* 14:392–398.

Crossley, A. C. 1978. The morphology and development of the *Drosophila* muscular system. *In* The Genetics and Biology of *Drosophila*. Vol. 2B. M. Ashburner and T. R. F. Wright, editors. Academic Press, New York. 499–560.

Falkenthal, S., V. P. Parker, W. M. Mattox, and N. Davidson. 1984. *Drosophila melanogaster* has only one myosin alkali light chain gene which encodes a protein with considerable amino acid homology to chicken myosin alkali light chains. *Mol. Cell. Biol.* 4:956–965.

Fyrberg,E., and C. Beall. 1990. Genetic approaches to myofibril form and function in *Drosophila*. *Trends Genet.* 6:126–131.

Fyrberg, E., C. C. Fyrberg, C. Beall, and D. L. Saville. 1990. *Drosophila melanogaster* troponin-T mutations engender three distinct syndromes of myofibrillar abnormalities. *J. Mol. Biol.* 216:657–675.

Giulian, G. G., R. L. Moss, and M. Greaser. 1983. Improved methodology for analysis and quantitation of proteins on one-dimensional silver-stained slab gels. *Anal. Biochem.* 129:277–287.

Giulian, G. G., R. L. Moss, and M. Greaser. 1984. Analytical isoelectric focusing using a high-voltage vertical slab polyacrylamide gel system. *Anal. Biochem.* 142:421–436.

Goldman, Y. E., and R. M. Simmons. 1984. Control of sarcomere length in skinned muscle fibres of *Rana temporaria* during mechanical transients. *J. Physiol. (Lond.).* 350:497–518.

Hiromi, Y., and Y. Hotta. 1985. Actin gene mutations in *Drosophila*; heat shock activation in the indirect flight muscles. *EMBO (Eur. Mol. Biol. Organ.) J.* 4:1681–1687.

Huxley, H. E. 1969. The mechanism of muscular contraction. *Science (Wash. DC).* 164:1356–1366.

Jewell, B. R., and J.C. Ruegg. 1966. Oscillatory contraction of insect fibrillar muscle after glycerol extraction. *Proc. R. Soc. Lond. Ser. B.* 164:428–459.

Karlik, C. C., and E. A. Fyrberg. 1985. An insertion within a variably spliced *Drosophila* tropomyosin gene blocks accumulation of only one encoded isoform. *Cell.* 41:57–66.

Kawai M., and P. W. Brandt. 1980. Sinusoidal analysis: a high resolution method for correlating biochemical reactions with physiological processes in activated skeletal muscles of rabbit, frog and crayfish. *J. Muscle Res. Cell Motil.* 1:279–303.

Kawai, M., and F. H. Schachat. 1984. Differences in the transient response of fast and slow skeletal muscle fibers. Correlations between complex modulus and myosin light chains. *Biophys. J.* 45:1145–1151.

Lehman, W., and A. G. Szent-Gyorgyi. 1975. Regulation of muscle contraction. Distribution of actin control and myosin control in the animal kingdom. *J. Gen. Physiol.* 66:1–30.

Leinhard, G. E., and I. I. Secemski. 1973. $P^1$, $P^5$-Di(adenosine-5')pentaphosphate, a potent multisubstrate inhibitor of adenylate kinase. *J. Biol. Chem.* 248:1121–1123.

Levine, J. 1973. Properties of the nervous system controlling flight in *Drosophila melanogaster*. *J. Comp. Physiol.* 85:129–166.

Lewis, E. B. 1960. A new standard food medium. *Drosophila Inform. Serv.* 34:117–118.

Lindlsey, D. L., and E. H. Grell. 1968. Genetic variations of *Drosophila melanogaster*. *Carnegie Inst. Wash.* Publ. 627.

Lindsley, D. L., and G. Zimm. 1985. The genome of *Drosophila melanogaster*, Part 1: genes A–K. *Drosophila Inform. Serv.* 62:1–227.

Lindsley, D. L., and G. Zimm. 1987. The genome of *Drosophila melanogaster*, Part 3: rearrangements. *Drosophila Inform. Serv.* 65:1–224.

Mahaffey, J. W., M. D. Coutu, E. A. Fyrberg, and W. Inwood. 1985. The flightless *Drosophila* mutant *raised* has two distinct genetic lesions affecting accumulation of myofibrillar proteins in flight muscles. *Cell.* 40:101–110.

Mogami, K., Y. Nonomura, and Y. Hotta. 1981. Electron microscopic and electrophoretic studies of a *Drosophila* muscle mutant wings-up B. *Jpn. J. Genet.* 56:51–65.

Mogami, K., S. C. Fugita, and Y. Hotta. 1982. Identification of *Drosophila* indirect flight muscle myofibrillar proteins by means of two-dimensional electrophoresis. *J. Biochem.* 91:643–650.

Mogami, K., P. T. O'Donnell, S. I. Bernstein, T. R. F. Wright, and C. P. Emerson, Jr. 1986. Mutations of the *Drosophila* myosin heavy-chain gene: effects on transcription, myosin accumulation and muscle function. *Proc. Natl. Acad. Sci. USA.* 83:1393–1397.

Molloy, J. E., V. Kyrtatas, J. C. Sparrow, and D. C. S. White. 1987. Kinetics of flight muscles from insects with different wing beat frequencies. *Nature (Lond.).* 328:449–451.

Moss, R. L., G. G. Giulian, and M. L. Greaser. 1982. Physiological effects accompanying the removal of myosin LC2 from skinned skeletal muscle fibers. *J. Biol. Chem.* 250:4007–4021.

Nachtigall, W., and D. M. Wilson. 1967. Neuromuscular control of *Dipteran* flight. *J. Exp. Biol.* 47:77–97.

Nave, R., and K. Weber. 1990. A myofibrillar protein of insect muscle related to vertebrate titin connects Z band and A band: purification and molecular characterization of invertebrate mini-titin. *J. Cell Sci.* 95:535–544.

O'Brien, S. J., and R. J. MacIntyre. 1978. Genetics and biochemistry of enzymes and specific proteins of *Drosophila*. *In* The Genetics and Biology of *Drosophila*, Vol. 2a. M. Ashburner and T. R. F. Wright, editors. Academic Press, New York. 395–551.

O'Donnell, P. T., and S. I. Bernstein. 1988. Molecular and ultrastructural defects in a *Drosophila* myosin heavy chain mutant: differential effects on muscle function produced by similar thick filament abnormalities. *J. Cell Biol.* 107:2601–2612.

Parker, V. P., S. Falkenthal, and N. Davidson. 1985. Characterization of the myosin light chain-2 gene of *Drosophila melanogaster*. *Mol. Cell. Biol.* 5:3058–3068.

Peckham, M., J. E. Molloy, J. C. Sparrow, and D. C. S. White. 1990. Physiological properties of the dorsal longitudinal flight muscle and the tergal depressor of the trochanter muscle of *Drosophila melanogaster*. *J. Muscle Res. Cell Motil.* 11:203–215.

Pirrotta, V., H. Steller, and M. P. Bozzetti. 1985. Multiple upstream regulatory elements control the expression of the *Drosophila* white gene. *EMBO (Eur. Mol. Biol. Organ.) J.* 4:3501–3508.

Pringle, J. W. S. 1978. The Croonian Lecture, 1977. Stretch activation of muscle: function and mechanism. *Proc. R. Soc. Lond. Ser. B.* 201:107–130.

Robertson, H. M., C. R. Preston, R. W. Phillis, D. M. Johnson-Schlitz, W. K. Benz, and W. R. Engels. 1988. A stable genomic source of P element transposase in *Drosophila melanogaster*. *Genetics.* 118:461–470.

Rubin, G. M., and A. C. Spradling. 1983. Vectors for P element mediated gene transfer in *Drosophila*. *Nucl. Acids Res.* 11:6341–6351.

Sanger, J. M., B. Mittal, M. B. Pochapin, and J. W. Sanger. 1986. Myofibrillogenesis in living cells microinjected with fluorescently labeled alpha-actinin. *J. Cell Biol.* 102:2053–2066.

Schaub, M. C., A. Jauch, D. Waizthoeny, and T. Wallimann. 1986. Myosin light chain functions. *Biomed. Biochem. Acta.* 45:539–544.

Shafiq, S. A. 1963. Electron microscopic studies on the indirect flight muscles of *Drosophila melanogaster*. II. Differentiation of myofibrils. *J. Cell Biol.* 17:363–373.

Sweeney, H. L., and J. T. Stull. 1990. Alteration of cross-bridge kinetics by myosin light chain phosphorylation in rabbit skeletal muscle: implications for regulation of actin-myosin interaction. *Proc. Natl. Acad. Sci. USA.* 87:414–418.

Takahashi, S., H. Takano-Ohmuro, and K. Maruyama. 1990. Regulation of *Drosophila* myosin ATPase activity by phosphorylation of myosin light chains–I. wild-type fly. *Comp. Biochem. Physiol.* 95B:179–181.

Tansey, T., M. D. Mikus, M. Dumoulin, and R. V. Storti. 1987. Transformation and rescue of a flightless *Drosophila* tropomyosin mutant. *EMBO (Eur.*

*Mol. Biol. Organ.) J.* 6:1375–1385.
Thorson, J., and D. C. S. White. 1983. Role of cross-bridge distortion in the small-signal mechanical dynamics of insect and rabbit striated muscle. *J. Physiol. (Lond.).* 343:59–84.
Toffenetti, J., D. Mischke, and M. L. Pardue. 1987. Isolation and characterization of the gene for myosin light chain two of *Drosophila melanogaster. J. Cell Biol.* 104:19–28.
Tregear, R. T. 1983. Physiology of insect flight muscle. *In* Handbook of Physiology. Section 10: Skeletal Muscle. L. D. Peachey, R. H. Adrian, and S. R. Geiger, editors. American Physiological Society, Bethesda, MD. 487–506.
Unwin, D. M., and C. P. Ellington. 1979. An optical tachometer for measurement of the wing-beat frequency of free-flying insects. *J. Exp. Biol.* 82: 377–378.
Vibert, P., and R. Craig. 1985. Structural changes that occur in scallop myosin filaments upon activation. *J. Cell Biol.* 101:830–837.
Victor, T., A. M. Jordaan, A. J. Bester, and A. Lochner. 1987. A sensitive and rapid method for separating adenine nucleotides and creatine phosphate by ion-pair reversed high-performance liquid chromatography. *J. Chromatogr.* 389:339–344.
Warmke, J. W. 1990. Genetic analysis of myosin light chain-2 function in *Drosophila melanogaster*. Ph.D. dissertation. The Ohio State University, Columbus.
Warmke, J. W., A. J. Kreuz, and S. Falkenthal. 1989. Co-localization to chromosome bands 99E1-3 of the *Drosophila melanogaster* myosin light chain-2 gene and a haploinsufficient locus that affects flight behavior. *Genetics.* 122:139–151.
White, D. C. S. 1983. The elasticity of relaxed insect fibrillar flight muscle. *J. Physiol. (Lond.).* 343:31–57.
White, D. C. S., J. Lund, and M. R. Webb. 1988. Cross-bridge kinetics in asynchronous insect flight muscle. *In* Advances in Experimental Medicine and Biology. Vol. 226. Molecular Mechanism of Muscle Contraction. H. Sugi and G. H. Pollack, editors. Plenum Press, New York. 169–178.
Wray, J. S. 1979. Filament geometry and the activation of insect flight muscles. *Nature (Lond.).* 280:325–326.
Yamakawa, M., J. Warmke, S. Falkenthal, and D. Maughan. 1991. Frequency analysis of skinned indirect flight muscle from a myosin light chain-2 deficient mutant of *Drosophila melanogaster* with a reduced wing beat frequency. *In* Proceedings of the Sixth Annual Research Symposium: Regulation of Smooth Muscle Contraction. Plenum Press, New York. 455–460.